Supervillin (p205): A Novel Membrane-associated, F-Actin–binding Protein in the Villin/Gelsolin Superfamily

Kersi N. Pestonjamasp, Robert K. Pope, Julia D. Wulfkuhle, and Elizabeth J. Luna

Worcester Foundation for Biomedical Research, an Affiliate of the University of Massachusetts Medical Center, Shrewsbury, Massachusetts 01545

Abstract. Actin-binding membrane proteins are involved in both adhesive interactions and motile processes. We report here the purification and initial characterization of p205, a 205-kD protein from bovine neutrophil plasma membranes that binds to the sides of actin filaments in blot overlays. p205 is a tightly bound peripheral membrane protein that cosediments with endogenous actin in sucrose gradients and immunoprecipitates. Amino acid sequences were obtained from SDS-PAGE–purified p205 and used to generate antipeptide antibodies, immunolocalization data, and cDNA sequence information. The intracellular localization of p205 in MDBK cells is a function of cell density and adherence state. In subconfluent cells, p205 is found in punctate spots along the plasma membrane and in the cytoplasm and nucleus; in adherent cells, p205 concentrates with E-cadherin at sites of lateral cell–cell contact. Upon EGTA-mediated cell dissociation, p205 is internalized with E-cadherin and F-actin as a component of adherens junctions "rings." At later times, p205 is observed in cytoplasmic punctae. The high abundance of p205 in neutrophils and suspension-grown HeLa cells, which lack adherens junctions, further suggests that this protein may play multiple roles during cell growth, adhesion, and motility. Molecular cloning of p205 cDNA reveals a bipartite structure. The COOH terminus exhibits a striking similarity to villin and gelsolin, particularly in regions known to bind F-actin. The NH_2 terminus is novel, but contains four potential nuclear targeting signals. Because p205 is now the largest known member of the villin/gelsolin superfamily, we propose the name, "supervillin." We suggest that supervillin may be involved in actin filament assembly at adherens junctions and that it may play additional roles in other cellular compartments.

Interactions between the plasma membrane and the actin cytoskeleton are involved in controlling cell shape, in organizing membrane proteins into domains, and in regulating membrane domain function (52). Some of these domains contain membrane-spanning proteins, such as ion channels and adhesion molecules, which are localized because of interactions with cortical meshworks of spectrin–cross-linked actin filaments (7, 27). Other actin-based membrane skeletons underlie membrane domains responsible for cell–substrate and cell–cell adhesion (64, 80). For instance, intercellular adhesion at adherens junctions, which is mediated by Ca^{2+}-sensitive transmembrane proteins called cadherins, depends upon cadherin attachment to actin filaments through linker proteins, such as α- and β-catenins (1). Similarly, indirect interactions between actin filaments and integrins, mediated through numerous other linker proteins in focal contacts, can regulate integrin binding to ligands in the extracellular matrix and thus affect cell–substrate adhesion (13, 87).

Membrane–actin linkages are also important for the assembly and control of more dynamic structures, e.g., pseudopods, filopodia, and microvilli (10, 19, 52, 55). For example, the actin-binding glycoprotein ponticulin (86) is required for pseudopod stabilization, efficient chemotaxis, and normal multicellular development of *Dictyostelium discoideum* amebae (42, 74). The *Dictyostelium* F-actin–bundling protein, p30a, also modulates the structure and function of cell surface extensions. This protein is concentrated in filopodia (29), stabilizes actin filaments at sites of cell–cell interaction (30), and is required for normal filopodial structure and function (67). The actin-bundling protein called drebrin may play a similar role in mammalian cells since overexpression in fibroblasts induces the formation of long cell extensions that are relatively resistant to actin destabilization by cytochalasin D (46, 72). Finally, the ezrin, radixin, and moesin (ERM)[1] proteins may help stabilize both adherens junctions and dynamic cell surface extensions (79). Simultaneous reduction of the intracellular levels of these structurally related, F-actin–

K.N. Pestonjamasp and R.K. Pope contributed equally to this work.

Address all correspondence to E.J. Luna, Worcester Foundation Campus, University of Massachusetts Medical Center, 222 Maple Avenue, Shrewsbury, MA 01545. Tel.: (508) 842-8921. Fax: (508) 842-3915. E-mail: LUNA@sci.wfbr.edu

1. *Abbreviations used in this paper*: ERM, ezrin, radixin, and moesin; ORF, open reading frame; RACE, rapid amplification of cDNA ends; TEB, Triton X-100 extraction buffer.

© The Rockefeller University Press, 0021-9525/97/12/1255/15 $2.00

binding proteins inhibits both cell–cell adhesion and the formation of microvilli, filopodia, and membrane ruffles (77).

One approach to the identification of proteins that bind actin at the plasma membrane is the use of ^{125}I-labeled F-actin blot overlays. This technique is particularly useful for identifying F-actin–binding proteins in membrane skeletons because such proteins, which are often difficult to solubilize, can be solubilized with SDS before analyzing for actin binding activity (17, 66). This approach has been used successfully to monitor the distribution and/or purification of ponticulin (17, 18), p30a (17, 36), drebrin (54), and the ERM proteins (66). Although it is not clear why this technique selectively identifies many membrane-associated, as opposed to strictly cytoplasmic, actin-binding proteins, this has proved to be true so far.

One membrane-associated protein that we have identified using F-actin blot overlays exhibits an apparent M_r of 205 on SDS–polyacrylamide gels. This protein (p205), which binds to the sides of actin filaments, is especially prominent in crude membranes from bovine neutrophils (66) and in whole cell extracts and crude membrane fractions from cervical carcinoma (HeLa) cells (54; our unpublished observations). Because p205 is not immunocrossreactive with antibodies against myosin II, fodrin, talin, or tensin (66), and because myosins I and V do not bind F-actin on blot overlays under our conditions (54), we have speculated that p205 may be a new actin-binding membrane protein (66).

In this study, we demonstrate that p205 is, in fact, a previously uncharacterized component of both the neutrophil and MDBK cell membrane skeletons. This protein is a tightly bound peripheral protein that cofractionates with β-actin and γ-actin from neutrophil plasma membranes under stringent conditions and colocalizes with E-cadherin at sites of adhesion between MDBK cells. In subconfluent MDBK cells, punctate staining also is observed throughout the cytoplasm and within the nucleus. Using amino acid sequences derived from SDS-PAGE–purified p205 and PCR-RACE (rapid amplification of cDNA ends), we obtained a series of overlapping clones that encode the complete p205 cDNA. The deduced protein sequence includes a COOH terminus that is very similar to the villin/gelsolin family of actin-binding proteins. The NH_2 terminus of p205 is novel and contains several potential nuclear localization signals. Based on the striking similarity with villin/gelsolin, p205 is apparently the largest known member of the villin superfamily, and accordingly, we suggest the name "supervillin." The primary sequence motifs and cellular localization(s) of supervillin suggest that this protein is a structural component of the plasma membrane skeleton that may also play a role in cell–cell adhesion and/or information transfer to other cell compartments.

Materials and Methods

Cell Culture

Cells were grown with 10% FBS unless otherwise specified. MDBK cells were grown in MEM with Earl's balanced salts; SHSY5Y human neuroblastoma cells in RPMI-1640; NIH-3T3 cells and COS-7 monkey kidney cells in DME; pig kidney epithelial cells (LLC-PK1) in medium 199 with 3% FBS; NRK cells in F-12 nutrient mixture; HeLa-S3 cells in Joklik MEM with 5% FBS (Irvine Scientific, Santa Ana, CA). The SHSY5Y neuroblastoma cells were a gift of Dr. A.H. Ross and the HeLa cells were provided by Dr. T. Pederson, both from the Worcester Foundation for Biomedical Research (Shrewsbury, MA). The remaining cell lines were obtained from the American Type Culture Collection (Rockville, MD). Reagents for tissue culture were purchased from GIBCO Laboratories (Grand Island, NY).

Neutrophils and Plasma Membranes

Neutrophils were isolated from 8 to 16 liters of fresh bovine blood by differential lysis, followed by fractionation on preformed gradients of isotonic Percoll (Pharmacia Biotechnology, Piscataway, NJ) and were disrupted by nitrogen cavitation (24, 60, 66). Plasma membranes, secretory vesicles, pooled granules, and cytosol were separated by flotation of the postnuclear supernatant into a step Percoll gradient (21). Briefly, cavitates were centrifuged to remove nuclei and mixed with an equal volume of a 1.12 g/ml Percoll solution in relaxation buffer (66). Gradients consisted of 5 ml of 1.12 g/ml Percoll in relaxation buffer, 14 ml of the cavitate/Percoll mixture, 14 ml of a 1.04 g/ml Percoll suspension in relaxation buffer, and 5 ml of relaxation buffer. After centrifugation at 65,000 *g* for 20 min at 4°C, the plasma membrane fraction was collected from the top of the 1.04 g/ml Percoll layer. Secretory vesicles were harvested from the interface between the 1.04 g/ml Percoll layer and the layer that initially contained cavitate. Pooled granules were collected from the bottoms of the centrifuge tubes. "Cytosol" was defined as the supernatant obtained after centrifuging the cavitate-containing layer at 141,000 *g* for 2 h at 4°C. The various membrane-containing fractions were centrifuged under the same conditions to remove Percoll, and the less-dense organellar pellets were resuspended in relaxation buffer and stored in aliquots at −80°C.

Electron Microscopy

Purity of the plasma membrane fraction was assessed by transmission electron microscopy. The plasma membrane and secretory vesicle fractions (0.5 ml each) were overlaid onto 2-ml cushions of 64% sucrose in relaxation buffer and centrifuged at 200,000 *g* for 30 min at 4°C to pellet residual Percoll. Membranes were collected from the tops of the sucrose cushions, diluted with relaxation buffer, and recentrifuged into a tight pellet at 200,000 *g* for 15 min at 4°C. The pellets were fixed for 1 h at 0°C in 2.5% glutaraldehyde, 0.1 M sodium cacodylate, pH 7.4, washed three times with cacodylate buffer, and then postfixed with 2% OsO_4, 0.1 M sodium cacodylate, pH 7.4. After three more washes with buffer, the pellets were stained en bloc with 0.5% aqueous uranyl acetate, dehydrated in ethanol/acetone, and then embedded in EMBED 812 - DER 736 (Electron Microscopy Sciences, Ft. Washington, PA). Sections of ~65 nm were cut both parallel and perpendicular to the axis of centrifugation and then stained with 5% aqueous uranyl acetate for 30 min and Reynolds' lead citrate for 30 s before visualization on an electron microscope (EM 301; Philips Electron Optics, Inc., Mahwah, NJ) at an accelerating voltage of 60 kV.

Membrane Extractions

Detergent extractions were carried out at 0°C for 60 min with either 1% Triton X-100, 3% octylglucoside, or 0.1% SDS in 1 mM EGTA, 2.5 mM MgATP, 0.3 μM aprotinin, 2 μM leupeptin, 3 μM pepstatin, 1 mM PMSF, 25 mM Tris-HCl, pH 7.5, and either 50, 150, or 250 mM NaCl. As a positive control, membranes were extracted at 70°C for 10 min with 1% SDS. Supernatants and pellets were collected after centrifugation at 200,000 *g* for 60 min.

For extraction with salt or alkali, plasma membranes were suspended in 20 mM sodium phosphate, pH 7.5, containing 1 mM EDTA, 1 mM DTT, and the above-mentioned protease inhibitors. Membranes were extracted at 0°C for 60 min with either 2.5 mM MgATP, 0.25 M KCl, 1.0 M KCl, or for 10 min in 0.1 M sodium carbonate or 0.1 M NaOH. Supernatants and pellets were collected after centrifugation at 200,000 *g* for 60 min through a 10% sucrose cushion prepared in the above buffer. Samples were denatured for 10 min at 70°C in Laemmli sample buffer before analysis on SDS-PAGE (51).

Phalloidin Shift Experiments

Plasma membranes (1 mg/ml), in the presence or absence of 10 μM phalloidin (Boehringer Mannheim GmbH, Mannheim, Germany), were extracted for 1 h at 0°C with Triton X-100 extraction buffer (TEB): 1% Triton X-100, 250 mM NaCl, 2.5 mM MgATP, 2 mM EGTA, 0.3 μM aprotinin, 2 μM leupeptin, 3 μM pepstatin, 1 mM PMSF, 25 mM Tris-HCl, pH 7.4. Samples (0.8 ml) were centrifuged at 200,000 *g* for 16 h at 4°C into 20–55%

linear sucrose gradients (3.6 ml) over a 64% sucrose cushion (0.5 ml). Fractions (0.3 ml) were collected from the top of the gradient with a density gradient fractionator (Isco, Lincoln, NE) and analyzed for the presence of cytoskeletal proteins after SDS-PAGE and electrotransfer to nitrocellulose (78). Calibration standards and accepted values (75) for Svedberg coefficients were: β-amylase (9 S), bovine thyroglobulin (19 S), and *Escherichia coli* small ribosomal subunit (30 S). Changes in the distribution of p205 were assessed by quantification of bound ^{125}I-labeled F-actin on overlays as described below.

Immunoblots and F-Actin Blot Overlays

Nitrocellulose blots were probed for moesin, ezrin, and p205 using ^{125}I-labeled F-actin (17, 66). Other cytoskeletal proteins were visualized with either monoclonal antibodies (β-actin) or polyclonal antibodies (γ-actin, fodrin, and myosin II). Dr. J.C. Bulinski (Columbia University College of Physicians and Surgeons, New York) generously supplied the antibody against γ-actin (63), and the antifodrin (nonerythroid spectrin) antibody (14) was a gift from Dr. K. Burridge (University of North Carolina, Chapel Hill, NC). Antibodies against β-actin and nonmuscle myosin II were obtained from Sigma Chemical Company (St. Louis, MO) and Biomedical Technologies, Inc. (Stoughton, MA), respectively. Polyclonal antibodies were visualized with 0.1 μCi/ml ^{125}I-labeled rProtein A™ (Dupont NEN, Boston, MA). Antibody against β-actin was visualized by incubating blots either with 0.25 μg/ml ^{125}I-labeled goat anti–mouse IgG (Amersham Corp., Arlington Heights, IL) or with 5 μg/ml rabbit anti–mouse IgG (Pierce Chemical Co., Rockford, IL), followed by incubation with ^{125}I-labeled rProtein A™. After exposure to film, relative amounts of labeled protein were quantified with a scanning densitometer (PDI, Huntington Station, NY).

Purification and Microsequencing of p205

Plasma membranes (160 mg) at a concentration of 1 mg/ml were extracted for 60 min at 0°C with TEB. After centrifugation at 141,000 *g* for 60 min, the pellet was solubilized by sonication for 1 min at 0°C (bath sonicator) in 10 ml of 4% SDS, 0.1 mM DTT, 10 mM Tris-HCl, pH 7.5, and heated for 10 min at 70°C. The suspension was clarified by centrifugation at 240,000 *g* for 30 min and concentrated to 3 ml in a Centricon-100 microconcentrator (Amicon, Bedford, MA). High molecular weight polypeptides were resolved by electrophoresis into a ~15-cm-long 5% SDS–polyacrylamide gel. When a visible myosin standard (Amersham Corp.) had migrated to ~10 cm, the proteins were electrotransferred onto a polyvinylidene difluoride (PVDF) membrane (Millipore Corp., Bedford, MA) and visualized by staining with Ponceau S. The band just under myosin, which corresponded to p205, was excised, washed extensively with sterile water, and then digested with either sequencing grade *N*-1-tosylamide-2-phenylethylchloromethyl ketone–trypsin (Promega Corp., Madison, WI) or Endo-LysC (Promega Corp.). Peptides were purified on a micropore HPLC and sequenced by Dr. J.D. Leszyk at the Worcester Foundation for Biomedical Research, W.M. Keck Protein Chemistry Facility (Shrewsbury, MA).

Anti-p205 Antibodies

Polyclonal antisera were generated against synthetic peptides corresponding to the two longest p205 sequences (SPVELDEDFDVIFDPYAPR and VPRPQTTAGDVLDGVN) by Research Genetics, Inc. (Huntsville, AL). Antipeptide antibodies were produced against each peptide (peptides A and B, respectively) after conjugation to keyhole limpet hemocyanin. ELISA titers (40) of antibodies directed against peptide A ranged from 108,600 to 300,000; titers of antibodies against peptide B were much lower (4,300–6,700). Antibodies were affinity purified against the cystinyl aminocaproic acid derivative of the appropriate peptide conjugated to immobilized chicken egg white lysozyme (47). IgG was purified by ammonium sulfate precipitation and DE52 chromatography (45) and was incubated overnight at 4°C with the appropriate affinity matrix. After extensive washes with PBS (150 mM NaCl, 10 mM sodium phosphate buffer, pH 7.5) and with 0.5 M NaCl, 10 mM Tris-HCl, pH 7.6, high affinity antipeptide antibodies were eluted with 3.5 M $MgCl_2$, 50 mM Tris-HCl, pH 7.2. These antibodies were immediately diluted with 1 mg/ml BSA, 10 mM Tris-HCl, pH 7.6, dialyzed against 150 mM NaCl, 10 mM Tris-HCl, pH 7.6, and concentrated and stored at −20°C in this buffer containing 50% glycerol.

Immunoprecipitations

For most experiments, p205 was immunoprecipitated with antibodies against peptide A, but some experiments also used antibodies against peptide B. To show that both peptides originated from p205, neutrophil plasma membranes (6 mg) were extracted with TEB, solubilized with 1% SDS (0.6 ml) at 70°C for 10 min and diluted 10-fold with RIPA buffer (150 mM NaCl, 1% NP-40, 0.5% sodium deoxycholate, 0.1% SDS, 50 mM Tris-HCl, pH 8.0) lacking SDS to generate a final concentration of 0.1% SDS. The suspension was clarified by centrifugation at 200,000 *g* for 30 min, preadsorbed for 3 h at 4°C with nonspecific rabbit IgG bound to protein A–agarose beads (Bio-Rad Laboratories, Hercules, CA) (31), and then centrifuged for 30 s at 100 *g*. p205 was precipitated from 0.5-ml aliquots of the supernatant by overnight incubation at 4°C with antisera and protein A–agarose beads. Controls employed either preimmune sera or immune sera in the presence of the appropriate competing peptide (66.6 μg/ml). Proteins bound to the agarose beads were sedimented through 1 M sucrose in RIPA buffer and solubilized with Laemmli sample buffer.

To demonstrate coimmunoprecipitation of actin with p205, neutrophil plasma membranes (1.0 mg/ml) were solubilized for 1 h at 0°C with TEB, preadsorbed, and then clarified, as described above. Clarified suspensions (0.25 ml) were incubated overnight at 4°C with protein A–agarose beads containing 150 μg of either affinity-purified antibodies against peptide A or nonspecific rabbit IgG. The beads were centrifuged for 3 min at 200 *g* through 1 M sucrose in TEB and washed three times with the high stringency RIPA buffer before solubilization for analysis by SDS-PAGE.

To demonstrate coprecipitation of p205 with actin, plasma membranes were treated briefly at 0°C with either fluorescein-phalloidin (Molecular Probes, Inc., Eugene, OR) or unlabeled phalloidin (Boehringer Mannheim GmbH) at a ratio of 1 μg of phalloidin/mg of membrane protein. Membranes (1 mg/ml) were extracted for 1 h at 0°C with TEB, preabsorbed, and clarified, as above. Clarified suspensions (0.45 ml) were incubated overnight at 4°C with protein A–agarose beads and 400 μg of either purified antifluorescein IgG (53) or nonspecific IgG. This amount of antifluorescein IgG is approximately equimolar to the amount of phalloidin bound to membrane actin. Beads were centrifuged through 1 M sucrose in TEB and solubilized in Laemmli sample buffer.

Immunofluorescence Microscopy

Confluent or subconfluent MDBK cells grown on coverslips were washed twice in PBS and fixed for 20 min at room temperature with PBS containing 1% EM grade formaldehyde (Electron Microscopy Sciences). EGTA-treated cells were washed with Dulbecco's PBS (138 mM NaCl, 2.7 mM KCl, 8.1 mM Na_2HPO_4, 1.2 mM KH_2PO_4, pH 7.0) and incubated at 37°C with 3 mM EGTA in the same buffer for 10, 20, and 30 min before fixation. After three washes with PBS, the fixed cells were permeabilized with 1% Triton X-100 in PBS for 1 min at room temperature, and then washed three more times. The coverslips were blocked with 10% horse serum, 1% BSA, and 0.02% sodium azide in PBS for ~2 h at room temperature or overnight at 4°C. Coverslips were then incubated 2–4 h at 37°C with either a monoclonal pan-cadherin antibody (Sigma Chemical Co.) diluted 1:1,000 in blocking solution, and/or affinity-purified antibodies against p205 peptide A at 150 μg/ml in blocking solution. After three washes in PBS, coverslips were incubated with a 1:750 dilution of Texas red–labeled, goat anti–rabbit IgG (Cappel Laboratories, Durham, NC) and/or a 1:1,000 dilution of Oregon green–labeled, goat anti–mouse IgG (Molecular Probes, Inc.) for 1 h at room temperature. In some experiments, the secondary antibody solution also contained 10 units/ml Bodipy-phallicidin (Molecular Probes, Inc.). At these antibody concentrations, no significant background was observed in the absence of primary antibody, and no bleed through fluorescence was detected in samples labeled singly with either primary antibody. After the final washes, samples were mounted with Slowfade-Light Antifade Medium (Molecular Probes, Inc.) and observed using a confocal microscope (MRC 1024; Bio-Rad Laboratories) equipped with LaserSharp Version 2.1A software.

Molecular Cloning

Cloning of the p205 Peptide A Sequence. Degenerate oligonucleotide primers (5′-CCIGTIGARYTIGAYGARGA-3′ and 5′-CKIGGIGCRTAIGGRTCRAA-3′) corresponding to 20 bp at each end of the p205 peptide A microsequence were used with Advantage KlenTaq polymerase (CLONTECH, Palo Alto, CA) in a touchdown thermal cycle reaction (OMN-E cycler; Hybaid Ltd., Long Island, NY) to amplify a 53-bp product from

MDBK cDNA. The cDNA was prepared using the Marathon cDNA Amplification Kit (CLONTECH), and mRNA made with the PolyATtract mRNA Isolation System IV (Promega Corp.) from total RNA prepared using Tri Reagent (Molecular Research Center, Cincinnati, OH). Products were cloned into the pGEM-T vector (Promega Corp.), and propagated in JM-109 chemically competent cells (Promega Corp.). Plasmids were purified by boiling minipreps (5), screened for inserts by digestion with AatII/PstI, and sequenced (Sequenase Version 2.0, Amersham Corp.), yielding the nondegenerate central nucleotides of the MDBK peptide A sequence.

3′-RACE. A degenerate oligonucleotide primer (5′-AGTTNGATGAGGATTTCGATGTCATTTTYGAYCC-3′) and the CLONTECH Marathon Adaptor Primer 1 (AP1) were used with KlenTaq enzyme mix in touchdown PCR program No. 1 (CLONTECH) to generate a 3-kb, 3′-RACE product from the double-stranded cDNA template. Correct clones were identified by digestion with AatII/PstI; sequencing verified the presence of known codons downstream of the primer.

5′-RACE. Primers designed initially from 3′-RACE products and subsequently from 5′-RACE products were used in two sequential rounds of 5′-RACE reactions with the CLONTECH AP1 primer and KlenTaq enzyme mix to generate overlapping clones corresponding to the full-length cDNA encoding p205. Gene-specific primers used in these reactions were 5′-CTCGCGGCCAGCATCTTCAGGG-3′, 5′-GATCTTCCCTCGCGGCCAGCATCTTCAGGG-3′, 5′-TCAAACGACTTCTCCATCTCCCTGAAGAGC-3′, or 5′-GTCAGGTTCTCCCTGCTCAGCAAATCTTT-3′. Reaction products were cloned into pGEM-T, and colonies were screened using a modification of a standard protocol (71). Briefly, nitrocellulose filters were placed onto plates containing 100–300 medium-sized colonies (1.0 mm diam) for 30 s, and holes were punched for alignment. Filters were denatured, neutralized twice, washed twice, air dried, stacked individually between sheets of aluminum foil, autoclaved (3 min to sterilize, 3 min to dry), and then screened for proper inserts with end-labeled oligonucleotides corresponding to sequences upstream of the gene-specific primer (5).

Gene-specific PCR. Nondegenerate oligonucleotide primers (5′-GAGCCAGGTCAACTTCAAATTCAGAAATG-3′ and 5′-TATTAAGGTAGAAAGGTGGATTCGCACAGA-3′) and the Expand Long Template PCR System (Boehringer Mannheim GmbH) were used in a touchdown PCR reaction with first strand MDBK cDNA. The cDNA was prepared with the SuperScript Preamplification System for First Strand cDNA Synthesis (GIBCO Laboratories) from mRNA prepared using the Poly(A)Pure mRNA Isolation Kit (Ambion, Austin, TX). The 5,198-bp product was ligated into pGEM-T and completely sequenced.

Sequence Determination and Comparison. Full-length and deletion constructs generated from internal AatII and PstI restriction sites were sequenced in both directions by primer walking at the Iowa State University DNA Sequencing and Synthesis Facility (Ames, IA). The final sequence encoding supervillin (p205) (these sequence data are available from GenBank/EMBL/DDBJ under accession No. AF025996) represents the consensus sequence from 18 overlapping cDNAs. For each nucleotide, 6–13 independently generated cDNAs were sequenced in both directions.

RNA Isolation and Northern Analysis. MDBK mRNA was isolated from log-phase and confluent cultures with the Poly(A)Pure mRNA Isolation Kit. For Northern analyses, 5 μg of polyadenylated (poly(A)$^+$) RNA and 5 μg of RNA molecular weight markers II (Ambion) were separated per lane on a 0.8% agarose–formaldehyde gel, transferred to Duralon filters (Stratagene, La Jolla, CA) by capillary blotting, and UV cross-linked to the membrane (28). The blots were stained with methylene blue to visualize the markers and rRNA bands, and then hybridized with a ^{32}P-labeled, random-primed probe (28) produced using the Prime-A-Gene kit (Promega Corp.), using as a template either a 659-bp HindIII/SacI fragment from the 5′ end of the p205 cDNA or a 465-bp AatII fragment from the 3′ end of the sequence.

Sequence Analysis. Predicted secondary structure was determined using the PeptideStructure subroutine in the Genetics Computer Group, Inc. (Madison, WI) sequence analysis software package. Percent identity and homology were assessed using the GAP and PileUp subroutines in this same package. GAP was used for individual, optimized sequence comparisons, and PileUp for multiple sequence alignments.

Results

p205 Is a Peripheral Plasma Membrane Protein

As detected by blot overlays with ^{125}I-labeled F-actin (17), moesin, ezrin, and a polypeptide with an M_r of 205,000 (p205) were previously described as major actin-binding proteins in a bovine neutrophil membrane fraction called the γ fraction (66). The γ fraction contains both large sheets of plasma membrane and "secretory vesicles," which are intracellular vesicles of similar density and composition that are believed to represent mobilizable intracellular stores of plasma membrane proteins involved in cell adhesion and other activation-associated surface processes (9). Taking advantage of a recently described technique for separating human neutrophil membranes containing latent vs. surface-exposed alkaline phosphatase (21), we found that the use of a modified Percoll gradient does indeed separate the γ fraction into two membrane populations (Fig. 1). The less dense fraction (density <1.04) is enriched in large membrane sheets with associated amorphous filamentous structures (Fig. 1 *A*) and corresponds to the peak of surface-exposed alkaline phosphatase (not shown). Thus, the less dense fraction appears to be mostly plasma membrane. The denser fraction (density between 1.04 and 1.06) corresponds to the peak of latent alkaline phosphatase (not shown) and contains predominantly small osmophilic vesicles (Fig. 1 *B*). These vesicles probably represent secretory vesicles although some mitochondria are also observed in this fraction. While large amounts of all three major F-actin–binding proteins (p205, ezrin, moesin) were found in the plasma membrane fraction (Fig. 1 *C*, lane *1*), the enrichment was greatest for p205 since ezrin and moesin also were present in the secretory vesicle (Fig. 1 *C*, lane *2*) and cytosolic (Fig. 1 *C*, lane *3*) fractions. As reported previously (66), no F-actin–binding proteins were observed in the pooled granule fraction. There was at least

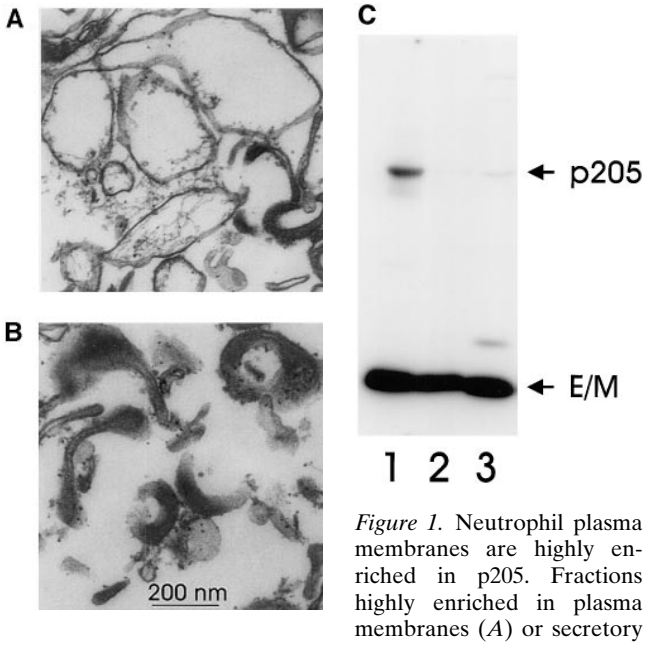

Figure 1. Neutrophil plasma membranes are highly enriched in p205. Fractions highly enriched in plasma membranes (*A*) or secretory vesicles (*B*) were analyzed for the presence of p205 by F-actin blot overlay (*C*). Aliquots (100 μg protein) were fractionated on a 5% SDS–polyacrylamide gel, transferred to nitrocellulose, and then probed with ^{125}I-labeled F-actin. Lane *1*, plasma membranes; lane *2*, secretory vesicles; and lane *3*, cytosol. *E/M*, the position of ezrin and moesin. Other cytosolic actin-binding proteins also are detected by this method (lane *3*).

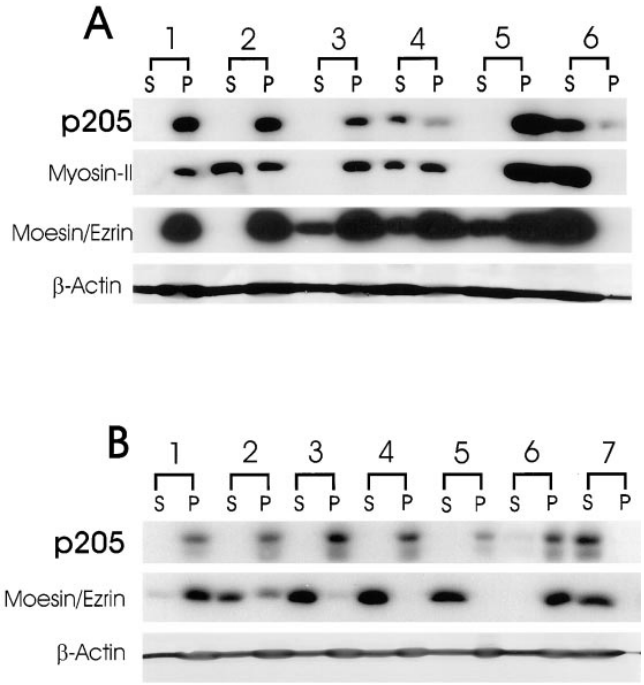

Figure 2. p205 is a peripheral component of the neutrophil plasma membrane skeleton. (*A*) Neutrophil plasma membranes were extracted with either buffer alone (lane *1*), or buffer containing a final concentration of 2.5 mM MgATP (lane *2*), 0.25 M KCl (lane *3*), 1.0 M KCl (lane *4*), 0.1 M sodium carbonate (lane *5*), or 0.1 M NaOH (lane *6*). For each extraction condition, high speed supernatants (*S*) and pellets (*P*) from 130-μg membranes were electrophoresed, blotted, and then probed with ^{125}I-labeled F-actin and with specific antibodies. (*B*) Neutrophil plasma membranes (100 μg per treatment) were extracted with either buffer alone (lane *1*), or buffer containing 1% Triton X-100 (lane *2*), 1% Triton X-100, 50 mM NaCl (lane *3*), 1% Triton X-100, 250 mM NaCl (lane *4*), 3% octylglucoside, 250 mM NaCl (lane *5*), or 0.1% SDS (lane *6*) and processed as above. A positive control consisted of membranes extracted with 1% SDS at 70°C for 10 min (lane *7*). The higher mobility F-actin–binding polypeptide present in *B* is consistently observed after detergent treatment; this band also reacts with an antibody against p205 sequences (see below), suggesting a close structural relationship with p205.

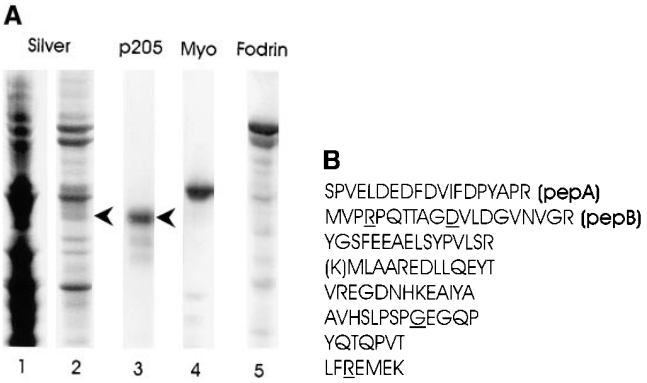

Figure 3. Purification of p205 by SDS-PAGE. (*A*) Neutrophil plasma membranes (lane *1*) and Triton X-100–insoluble pellets (lanes *2–5*) were separated on a 5% polyacrylamide gel and stained with silver (lanes *1* and *2*), or electrotransfered to nitrocellulose and probed with either ^{125}I-labeled F-actin (lane *3*), or with antibodies against myosin II (lane *4*), or nonerythroid spectrin/fodrin (lane *5*). Loads represent 100 μg membranes or equivalent amounts of Triton X-100–insoluble pellets. The location of p205 is indicated (*arrowheads*). (*B*) Eight microsequences were obtained from proteolytic digests of SDS-PAGE–purified p205. Polyclonal rabbit antibodies were generated against synthetic peptides corresponding to two of these sequences (*pepA* and *pepB*). Residues at variance with the deduced amino acid sequence (Fig. 11 *A*) are underlined; a lysine deduced from the cleavage specificity of Endo-LysC is shown in parentheses.

20-fold more p205 in the plasma membrane fraction than in the secretory vesicle fraction, and 10–15-fold more than in cytosol. This large enrichment suggests an intimate association of p205 with the plasma membrane.

To explore the nature of the interaction between p205 and the plasma membrane, we extracted purified neutrophil plasma membranes with a series of salt and detergent solutions (Fig. 2). We found that buffers containing 2.5 mM MgATP, a reagent that extracts most of the similarly sized myosin II, had no effect on the membrane association of p205 (Fig. 2 *A*, lanes *2S* and *2P*). Similarly, moderately high salt concentrations (0.25 M) that extract significant amounts of membrane-bound moesin and ezrin, had no detectable effect on the extractability of p205 (Fig. 2 *A*, lanes *3S* and *3P*). Even sodium carbonate, a reagent that extracts many peripherally bound proteins (44), had no effect on the membrane association of p205 (Fig. 2 *A*, lanes *5S* and *5P*). On the other hand, p205 was partially extracted at salt concentrations >1 M (Fig. 2 *A*, lanes *4S* and *4P*) and was almost completely extracted by 0.1 M NaOH (Fig. 2 *A*, lanes *6S* and *6P*), indicating that p205 is a tightly bound peripheral protein, and not an integral component, of the plasma membrane.

In agreement with this assessment, p205 also was resistant to extraction by a number of nonionic detergents (Fig. 2 *B*). At salt concentrations up to 250 mM, p205 remained insoluble in the presence of 1% Triton X-100 (Fig. 2 *B*, lanes *2–4*), 3% octylglucoside (Fig. 2 *B*, lanes *5S* and *5P*), or 0.1% SDS (Fig. 2 *B*, lanes *6S* and *6P*). The only detergent that effectively solubilized p205 was 1% SDS (Fig. 2 *B*, lanes *7S* and *7P*). Interestingly, a large fraction of the membrane-associated actin was retained in the p205-enriched pellet after extraction with buffers containing 250 mM NaCl and either 1% Triton X-100 or 3% octylglucoside (Fig. 2 *B*, lanes *4* and *5*), conditions that extracted essentially all moesin and ezrin. Thus, both p205 and actin appear to be detergent-resistant components of a membrane skeleton that does not require either moesin or ezrin for at least some of its integrity.

p205 Is a Previously Uncharacterized Protein

The inextractability of p205 under conditions that solubilized most membrane and membrane skeleton proteins, in conjunction with the large amounts of plasma membrane obtainable from bovine neutrophils, suggested that this protein should be readily purified by differential extraction followed by preparative SDS-PAGE. We thus extracted plasma membranes with a buffer containing 1% Triton X-100, 0.25 M NaCl, and 1 mM MgATP to identify proteins that are tightly associated with the neutrophil plasma membrane skeleton (Fig. 3 *A*, lane *2* vs. lane *1*).

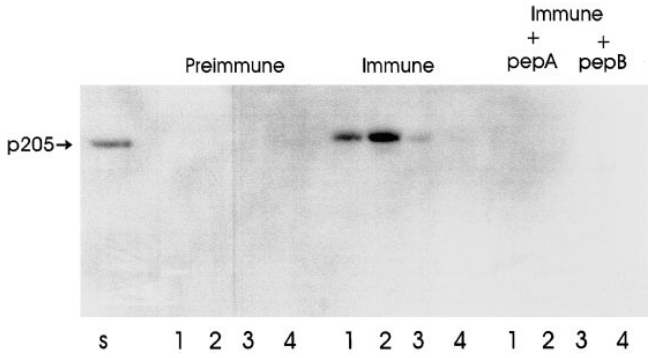

Figure 4. F-actin blot overlay shows that p205 is specifically immunoprecipitated from bovine neutrophil plasma membranes by antibodies against p205 peptides, pepA, and pepB. Proteins were immunoprecipitated from SDS-solubilized, Triton X-100–insoluble pellets by preimmune (*Preimmune*) or immune (*Immune*) sera from four different rabbits (lanes *1–4*) that were immunized with either peptide A (lanes *1* and *2*) or peptide B (lanes *3* and *4*). Antibody specificity is indicated by the absence of p205 from immunoprecipitates generated either with preimmune sera or with immune sera plus the appropriate competing peptide (*Immune* + *pepA*/*pepB*). *S*, p205 in the initial RIPA supernatant.

The inclusion of MgATP in this buffer resulted in the removal of most of the myosin II that migrated near p205 on SDS gels. When run on a long, 5% polyacrylamide gel, there was a clear separation of p205 from residual myosin and other similarly sized membrane skeleton proteins (Fig. 3 *A*, lanes *2–5*). Microsequencing of the band corresponding to p205 generated a total of eight peptide sequences (Fig. 3 *B*). None of these peptide sequences were significantly similar to any protein sequence in the nonredundant, updated protein databases, indicating that p205 is a previously uncharacterized protein.

To confirm that the peptide sequences in Fig. 3 *B* were derived from the F-actin–binding polypeptide called p205, antibodies against the two longest peptides (pepA, pepB) were used to specifically immunoprecipitate p205 from neutrophil membrane extracts (Fig. 4). Although pepA was much more immunogenic than pepB, antisera against either peptide, generated in each of four rabbits (Fig. 4, lanes *1–4*, respectively), specifically immunoprecipitated p205 from SDS- and heat-denatured membrane extracts (Fig. 4, *center*, lanes *1–4*). Specificity was indicated by the absence of p205 from immunoprecipitates generated with preimmune sera (Fig. 4, *left*) or with immune sera in the presence of the appropriate peptide antigen (Fig. 4, *right*). Similar results were obtained with the corresponding affinity-purified antibodies (data not shown). Thus, both pepA and pepB are derived from p205.

p205 Associates with Actin Filaments In Vivo

The high speed centrifugations used in the extraction experiments (Fig. 2) were expected to sediment essentially all membrane vesicles and large protein complexes. To determine whether p205 and endogenous β-actin sedimented together in the same detergent- and salt-resistant protein complex, we used the phalloidin shift assay originally described by Carraway and colleagues (15). In this approach, membranes are extracted with a Triton X-100–containing

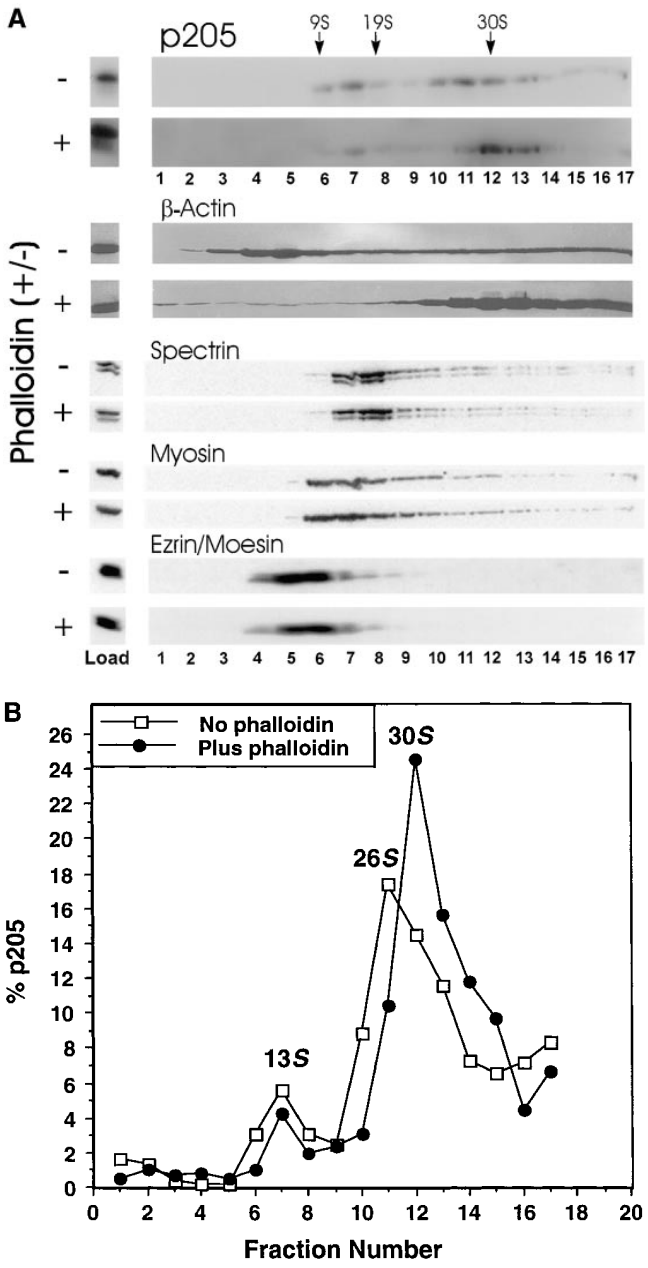

Figure 5. Treatment of membranes with phalloidin increases the sedimentability of p205, as well as actin. (*A*) Neutrophil plasma membranes treated without (−) or with (+) phalloidin were solubilized in TEB and fractionated on 20–55% sucrose gradients. The initial membrane extract (*Load*) and gradient fractions (lanes *1–17*) were analyzed for the presence of cytoskeletal proteins as described in Materials and Methods. Positions of calibration standards (*9S*, *19S*, and *30S*) are indicated. (*B*) Phalloidin-induced shift in the sedimentability of p205. Average distribution of p205 in gradient fractions, expressed as a percent of the total F-actin binding at 205 kD on F-actin blot overlays ($n = 3$). Similar results were observed when blot strips were re-probed with anti-pepA antibody, indicating that a single 205-kD F-actin–binding polypeptide is present in the 13S, 26S, and 30S complexes.

buffer in the presence and absence of 10 μM phalloidin. Microfilament-associated proteins are those that exhibit increased S values when sedimented in the presence of stabilized (plus phalloidin) vs. destabilized (no phalloidin) ac-

tin filaments. In our version of this assay, we used a buffer containing relatively high concentrations of Triton X-100 (1%), NaCl (250 mM), and MgATP (2.5 mM) to depolymerize significant amounts of the total actin and to dissociate most membrane skeleton proteins.

As expected for an F-actin–binding protein, p205 exhibited a reproducible phalloidin-induced increase in S value in TEB extracts of neutrophil plasma membranes (Fig. 5). In the presence of phalloidin, p205 sedimented as a component of a ~30 S complex (Fig. 5, *A* and *B*) that also contained the bulk of the membrane-associated β-actin (Fig. 5 *A*) and γ-actin (data not shown). Although variable amounts of a ~13 S moiety were observed in two experiments, most p205 sedimented as a ~26 S complex in the absence of phalloidin (Fig. 5 *B*). Surprisingly, whereas much of the actin was rendered monomeric by the harsh buffer conditions, significant amounts continued to sediment with high S values in the absence of phalloidin stabilization (Fig. 5 *A*). In contrast to the behavior of p205 and actin, little or no fodrin, myosin, ezrin, or moesin exhibited significant phalloidin-induced shifts in sedimentability under these conditions (Fig. 5 *A*). Thus, p205 apparently forms large complexes with endogenous actin under conditions that suggest an extremely tight association, direct or indirect, in the neutrophil membrane skeleton.

More evidence for the association of p205 with actin in situ was obtained by demonstrating that p205 and F-actin cosediment in reciprocal immunoprecipitation assays (Fig. 6, *A* and *B*). Because antiactin antibodies were less than optimal in these assays, we developed a procedure in which high affinity polyclonal antibodies against fluorescein (53, 83) were used to pellet actin filaments stabilized with fluorescein-labeled phalloidin. Neutrophil plasma membranes were incubated with fluorescein-phalloidin, and then phalloidin-bound actin filaments were precipitated from detergent-solubilized extracts with antifluorescein IgG (see Materials and Methods). Essentially all of the p205 in the initial extract (Fig. 6 *A*, lane *1*) coprecipitated with F-actin bound to fluorescein-phalloidin (Fig. 6 *A*, lane *3*), whereas little or no p205 was found in control experiments with nonspecific IgG (Fig. 6 *A*, lane *2*) or with unlabeled phalloidin (Fig. 6 *A*, lane *4*).

In converse experiments, we found that actin copelleted with p205 immunoprecipitated with affinity-purified antibodies against pepA (Fig. 6 *B*, lane *2*). Less than 5% as much actin coprecipitated with equivalent amounts of nonspecific IgG under these conditions (Fig. 6 *B*, lane *1*). Thus, both the phalloidin shift experiments and the coimmunoprecipitation assays suggest that the direct association between p205 and rabbit α-actin observed on F-actin blot overlays (Figs. 3 and 4; [66]) also occurs between p205 and actin on the neutrophil plasma membrane.

p205 Is Present in Many Cell Types

Based on immunoblot analyses with affinity-purified antibodies against p205, this protein is present in a number of cell types (Fig. 7). Both human cervical carcinoma cells (Fig. 7, *A* and *B*, lane *1*) and bovine kidney epithelial cells (Fig. 7 *A*, lane *2*; and *B*, lane *4*) contained at least as much p205 as bovine neutrophils (Fig. 7 *A*, lane *3*). The anti-pepA antibody was highly specific for p205 in these tissue

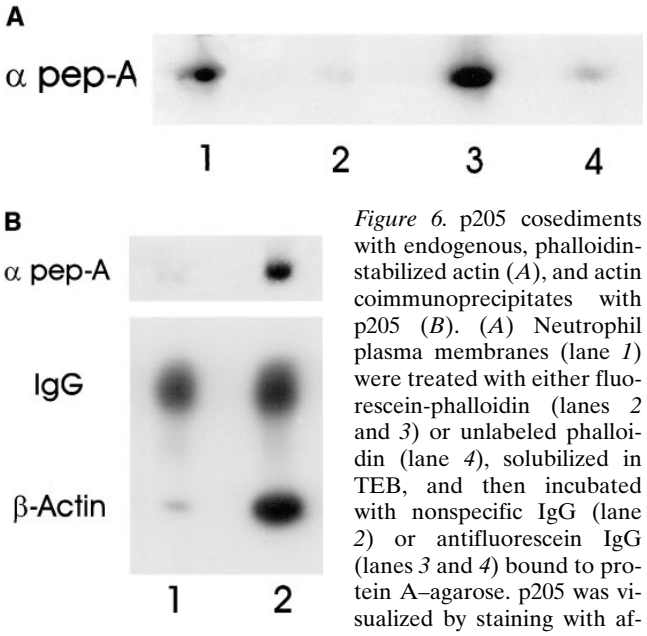

Figure 6. p205 cosediments with endogenous, phalloidin-stabilized actin (*A*), and actin coimmunoprecipitates with p205 (*B*). (*A*) Neutrophil plasma membranes (lane *1*) were treated with either fluorescein-phalloidin (lanes *2* and *3*) or unlabeled phalloidin (lane *4*), solubilized in TEB, and then incubated with nonspecific IgG (lane *2*) or antifluorescein IgG (lanes *3* and *4*) bound to protein A–agarose. p205 was visualized by staining with affinity-purified pepA IgG and by F-actin blot overlays (not shown). (*B*) IgG and actin in immunoprecipitates generated with either nonspecific rabbit IgG (lane *1*) or affinity-purified, anti-pepA antibody (lane *2*) after three washes with RIPA buffer. The relative amounts of actin cited in the text were normalized by reference to the amounts of IgG visualized by labeling with radiolabeled secondary IgG.

culture cells since they lacked a ~90-kD immunocrossreactive protein (Fig. 7 *A*, *arrowhead*) that is present in whole neutrophil extracts and pooled granules, but absent from purified neutrophil plasma membranes (data not shown). Other transformed and nontransformed cell lines also contained a 205-kD band recognized by both affinity-purified, anti-pepA antibodies (Fig. 7 *B*, *top*) and ^{125}I-labeled F-actin (Fig. 7 *B*, *bottom*). For instance, p205 was present in neuroblastoma SHSY5Y cells (Fig. 7 *B*, lane *2*), in 3T3 fibroblasts (Fig. 7 *B*, lane *3*), and in a number of epithelial cell lines (Fig. 7 *B*, lanes *4*–*7*). Although the affinity-purified pepA antibodies appeared to be specific for p205 in these cells, a second polypeptide with a slightly slower mobility was observed in F-actin blot overlays of 3T3 mouse (Fig. 7 *B*, lane *3*) and normal rat kidney (Fig. 7 *B*, lane *5*) cells. Thus, while p205 is found in many cell types, it is not the only protein in this size range that can be visualized by ^{125}I-labeled F-actin on blot overlays.

p205 Localization in Epithelial Cells

As was the case in neutrophils (Fig. 1), p205 was associated with plasma membranes in HeLa (not shown) and MDBK (Figs. 8–10) cells. First, p205 was enriched ~10-fold, about the same fold enrichment as a biotin cell surface marker, in crude plasma membrane fractions (4) from all three cell types (not shown). Second, immunofluorescence localization with affinity-purified, anti-pepA antibodies showed label at the plasma membrane in both low density (Fig. 8) and confluent (Fig. 9) MDBK cells. Low density cells (Fig. 8, *A* and *C*) and subconfluent cells (Fig. 9 *A*) also contained appreciable amounts of signal in punctate dots throughout the cytoplasm and within the nucleus. In

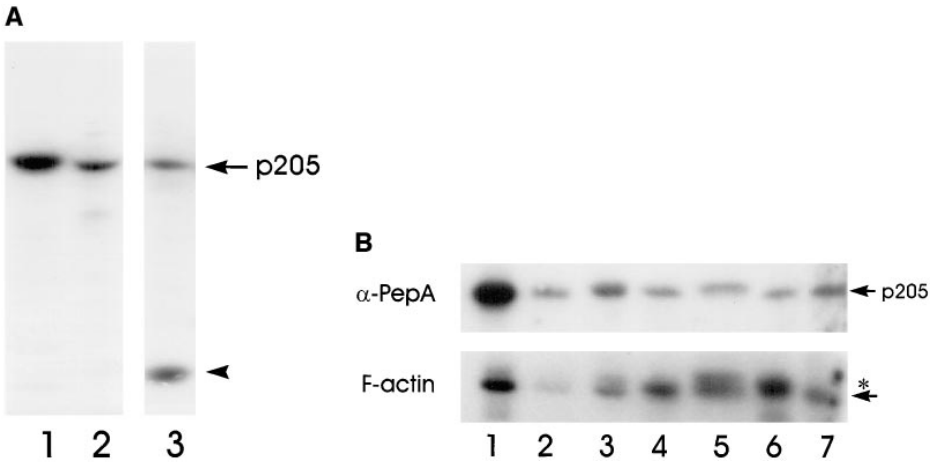

Figure 7. p205 is present in many cell types but is not the only ~205-kD F-actin–binding protein. (*A*) Nitrocellulose blots of HeLa cells (lane *1*), MDBK cells (lane *2*), and bovine neutrophils (lane *3*) stained with affinity-purified anti-pepA antibodies. Only the neutrophils contain a cross-reactive protein at ~90 kD (*arrowhead*). This 90-kD protein cofractionates with pooled neutrophil granules (66), specialized vesicles involved in host defense, and is distinct from the ~90-kD cytosolic actin-binding protein in Fig. 1 *C*, lane *3*. (*B*) Blots of HeLa (lane *1*), SHSY5Y neuroblastoma (lane *2*), 3T3 (lane *3*), MDBK (lane *4*), NRK (lane *5*), LLC-PK1 (lane *6*), and COS-7 cells (lane *7*) were stained in parallel with antibodies to pepA and F-actin. A higher molecular mass protein that binds F-actin, but not anti-pepA, is observed in lanes *3* and *5* (*).

nonjunctional regions of the plasma membrane, p205 staining was definite, but not pronounced, and did not necessarily colocalize with antibody against the cell–cell adhesion protein, E-cadherin (Figs. 8 and 9, *hollow arrows*). As the MDBK cells became confluent, the ratio between the plasma membrane and the internal p205 signal increased, as did the colocalization with E-cadherin at sites of both initial (Fig. 8, *C* and *D*) and established (Fig. 9, *A* and *B*) cell–cell contact (*solid white arrows*). In confluent cells, nearly all of the p205 staining was concentrated at lateral cell borders (Fig. 9 *C*), where it colocalized almost perfectly at the light level with E-cadherin (Fig. 9 *D*). Because

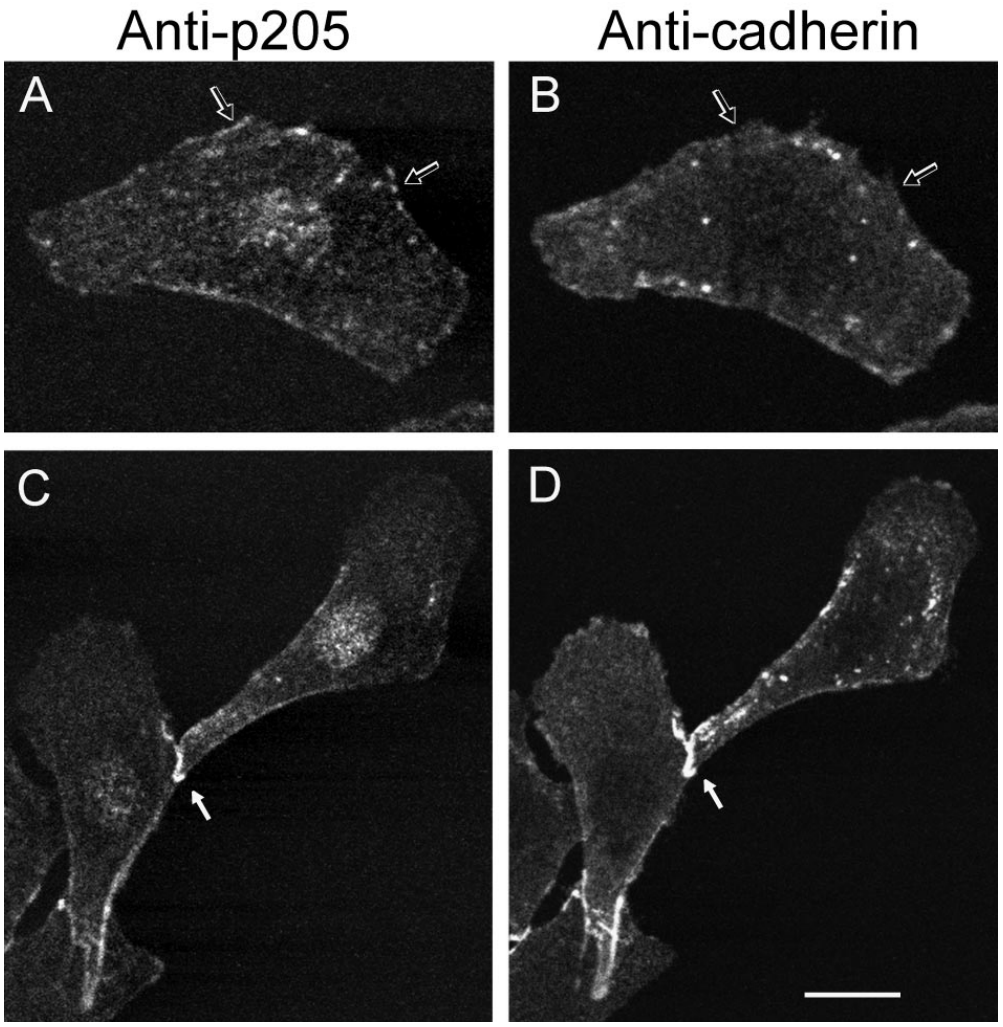

Figure 8. Distribution of p205 (*A* and *C*) and E-cadherin (*B* and *D*) in MDBK cells grown at low cell density. Cells were double labeled with affinity-purified, rabbit anti-pepA IgG and with monoclonal anticadherin antibodies, as described in Materials and Methods. Regions of p205 and cadherin colocalization at the plasma membrane (*white arrows*), and regions of anti-pepA staining alone (*hollow arrows*) are indicated. Bar, 10 μm.

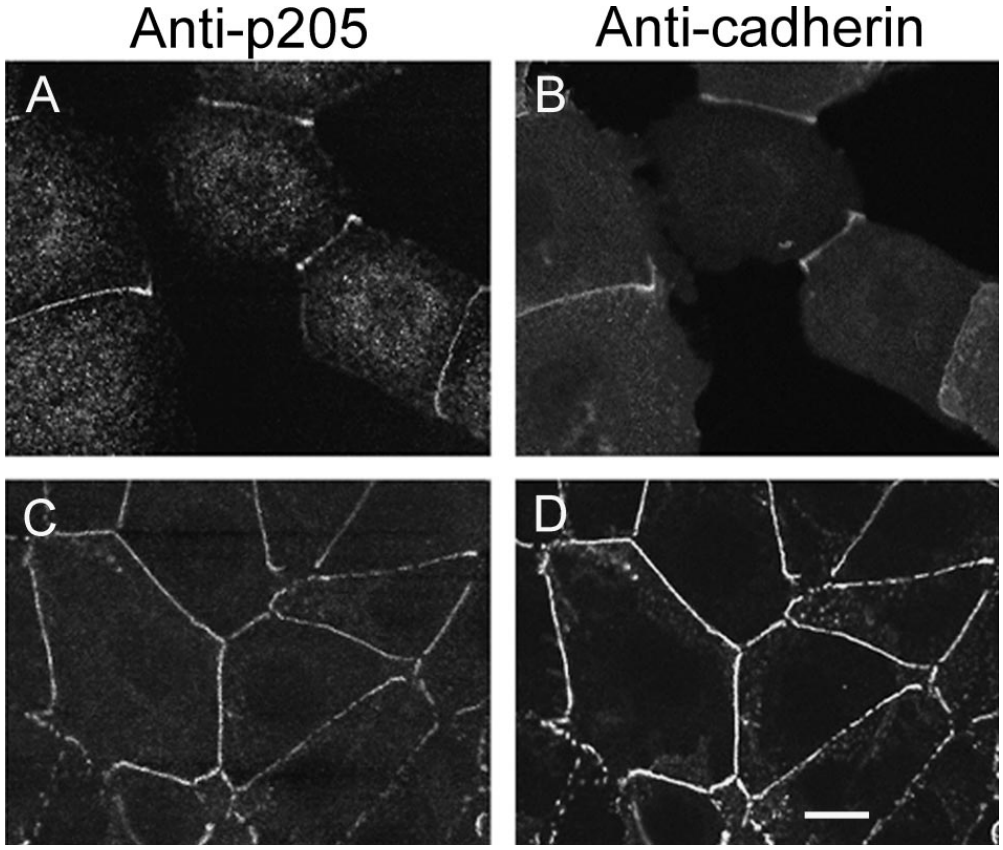

Figure 9. Distribution of p205 (*A* and *C)* and E-cadherin *(B* and *D*) in MDBK cells grown to high cell density. Cells were double labeled with affinity-purified, rabbit anti-pepA IgG and with monoclonal anticadherin antibodies. Regions of p205 and cadherin colocalization at the plasma membrane (*white arrows*) and regions of anti-pepA staining alone (*hollow arrows*) are indicated. Bar, 10 μm.

p205 staining was not observed in apical microvilli, nor with actin meshworks at basal cell surfaces (not shown), we infer that the colocalization with cadherin-containing, adherens-type junctions is specific and may reflect a role for p205 in the formation or stabilization of these structures.

To explore further the extent of the association between p205 and cadherin-containing junctional complexes, confluent monolayers of MDBK cells were treated with 3 mM EGTA, which induces the release of intercellular contacts and a coordinate internalization of vesicles containing E-cadherin and bound junctional proteins (49). At early times after treatment with EGTA, p205 (Fig. 10 *A*) colocalized with ringlike structures of bundled actin filaments (Fig. 10 *B*) and E-cadherin (not shown) during their contraction into the cytoplasm away from the membrane (49, 82). At later times after EGTA-mediated cell–cell dissociation, p205 (Fig. 10 *C*) and E-cadherin (Fig. 10 *D*) continued to colocalize in fragmented barlike structures near the nucleus. As these structures broke down with time (49, 82), p205 became dissociated into cytoplasmic punctae (Fig. 10 *E*) that no longer colocalized significantly with the large juxtanuclear structures containing cadherin (Fig. 10 *F*). However, p205 and cadherin continued to colocalize at sites of residual cell–cell contact (Fig. 10, *E* and *F*). No significant intranuclear staining for either p205 or cadherin was observed at any time after addition of EGTA.

These results indicate an extensive association, direct or indirect, between E-cadherin, p205, and F-actin in adherens-type junctions and suggest that p205 also can reside in a separate, punctate cytoplasmic compartment, e.g., on vesicles. These observations further suggest that the nuclear signal observed in low density cells (Fig. 8, *A* and *C*) may represent yet another p205-containing intracellular compartment. On the other hand, the preponderance of nuclear staining artifacts in immunofluorescence microscopy (57) remains an important caveat.

Molecular Cloning of p205

Primers with both inosines and degeneracies were designed from each end of the pepA microsequence (Fig. 3 *B*) and used in a PCR reaction to obtain the nondegenerate central portion of the pepA sequence (see Materials and Methods). Once the central region of the pepA sequence was known, primers designed from this sequence were used in a 3′-RACE reaction with oligo-dT primed cDNA to obtain four 3-kb clones corresponding to the 3′ end of the p205 cDNA (Fig. 11 *A*, *right arrows*). Nondegenerate primers designed from these sequences were used in a 5′-RACE reaction to generate five clones containing 5′ sequences. A second round of 5′-RACE with new primers was used to ensure that the 5′ end of the p205 cDNA had been identified. A total of six clones were obtained that all begin at the same nucleotide (Fig. 11 *A*, *left arrows*). As a check for cDNA production artifacts, two gene-specific primers were used to generate 5,198-bp clones that contained most of the p205 coding sequence (Fig. 11 *A*, *no arrows*). Products of this size were obtained from two different commercial cDNA libraries (data not shown).

To confirm the approximate message size, Northern analysis was performed with MDBK poly(A)$^+$ RNA (Fig. 11 *B*). Both a probe from the 5′ end of the sequence (Fig. 11 *A*, *probe 1*) and a probe from the 3′ half of the se-

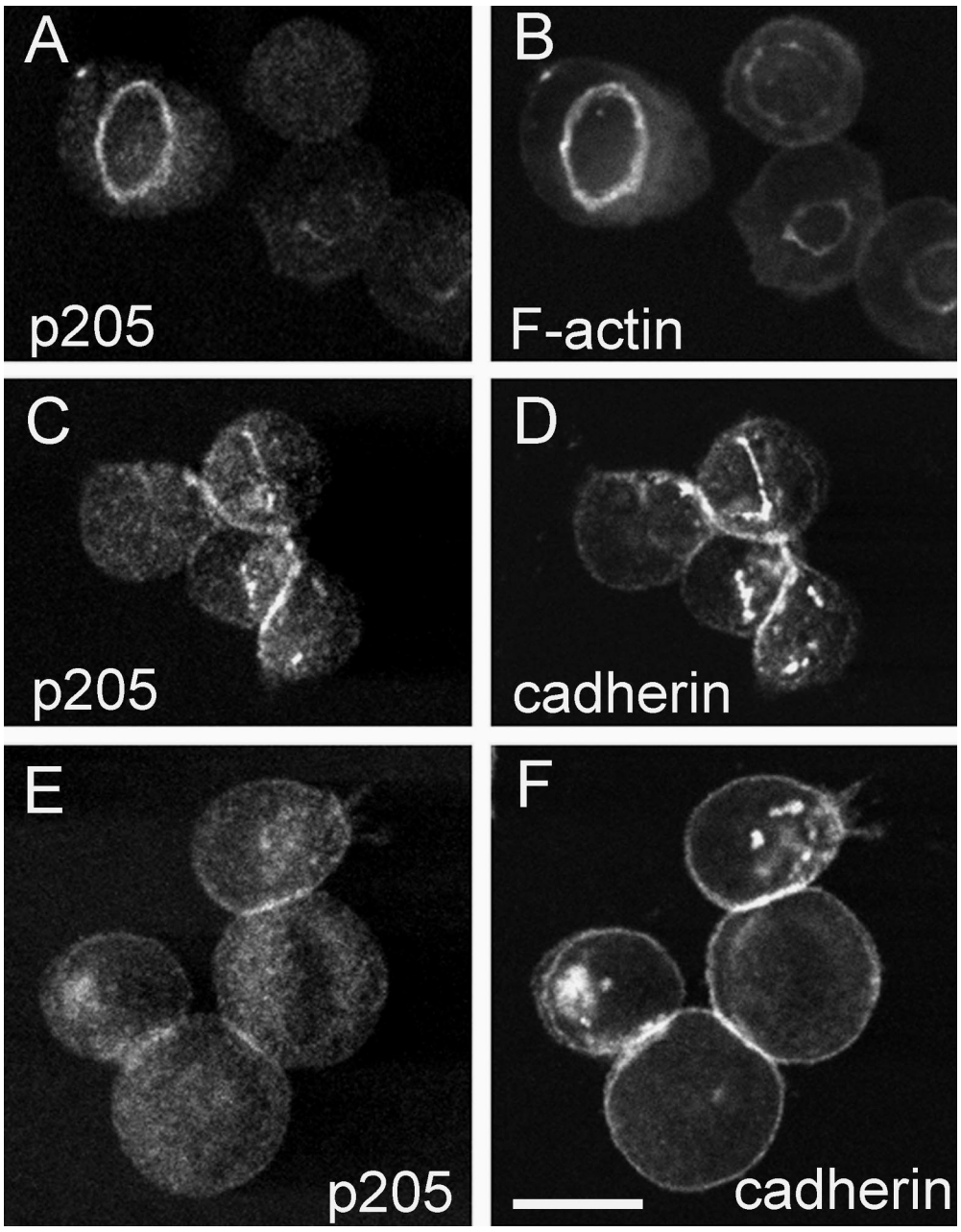

Figure 10. Colocalization of p205 (*A*, *C*, and *E*) with F-actin (*B*) and cadherin (*D* and *F*) in ringlike structures and cytoplasmic aggregates 10 min after EGTA treatment to disrupt cell adhesions. After 30 min (*E* and *F*), most of the cadherin is dissociated from p205, which is diffusely distributed in cytoplasmic puncta. Cells were double labeled with affinity-purified pepA antibodies and either fluorescein-phalloidin or anticadherin antibodies. Bar, 10 μm.

quence (Fig. 11 *A*, *probe 2*) recognized a ~7.2-kb message in MDBK cells (Fig. 11 *B*, lanes *1* and *2*). This message size is consistent with the ~6.5-kb cDNA obtained by PCR, given the presence of a poly(A)$^+$-tail of unknown size. A third probe near the 5′ end of the sequence showed a single ~7.2-kb band on Northern blots (data not shown). The source of the ~1.8-kb band visualized with probe 2 (Fig. 11 *B*, lane *2*) is not known, but this band comigrates with residual 18 S rRNA.

Primary Structure of p205

The consensus DNA sequence encoded a protein of 1,792 amino acids (Fig. 12 *A*) that is absent from current protein databases. The predicted mol wt of 200,626 (isoelectric point ~6.44) (8) is in good agreement with that predicted for p205 by SDS-PAGE (Fig. 1). Relative to an "average" protein (20), p205 is high in arginine (7.1% vs. 4.7%) and glutamine (9.2% vs. 6.2%) and low in tyrosine (2.3% vs. 3.5%) and cysteine (1.3% vs. 2.8%), variations that are consistent with its relative insensitivity to staining by silver (Fig. 3 *A*) (62). The deduced amino acid sequence includes all eight peptides obtained from purified p205 (Figs. 3 *B* and 12 *A*, *double underlines*). Since antibodies against two of these peptides immunoprecipitate the F-actin–binding protein of ~205,000 D from SDS-solubilized neutrophil plasma membranes (Fig. 4), the sequence in Fig. 12 *A* undoubtedly encodes p205.

Analysis of the deduced amino acid sequence suggests that p205 is a bipartite protein with distinctly different NH_2- and COOH-terminal domains (Fig. 12 *B*). The NH_2-terminal half (first ~935 amino acids) contains numerous charge clusters in the context of a primarily α-helical secondary structure. One 17-residue motif and three short clusters of positively charged amino acids (Fig. 12 *A*, *gray boxes*) fit the consensus sequences for, respectively, nucle-

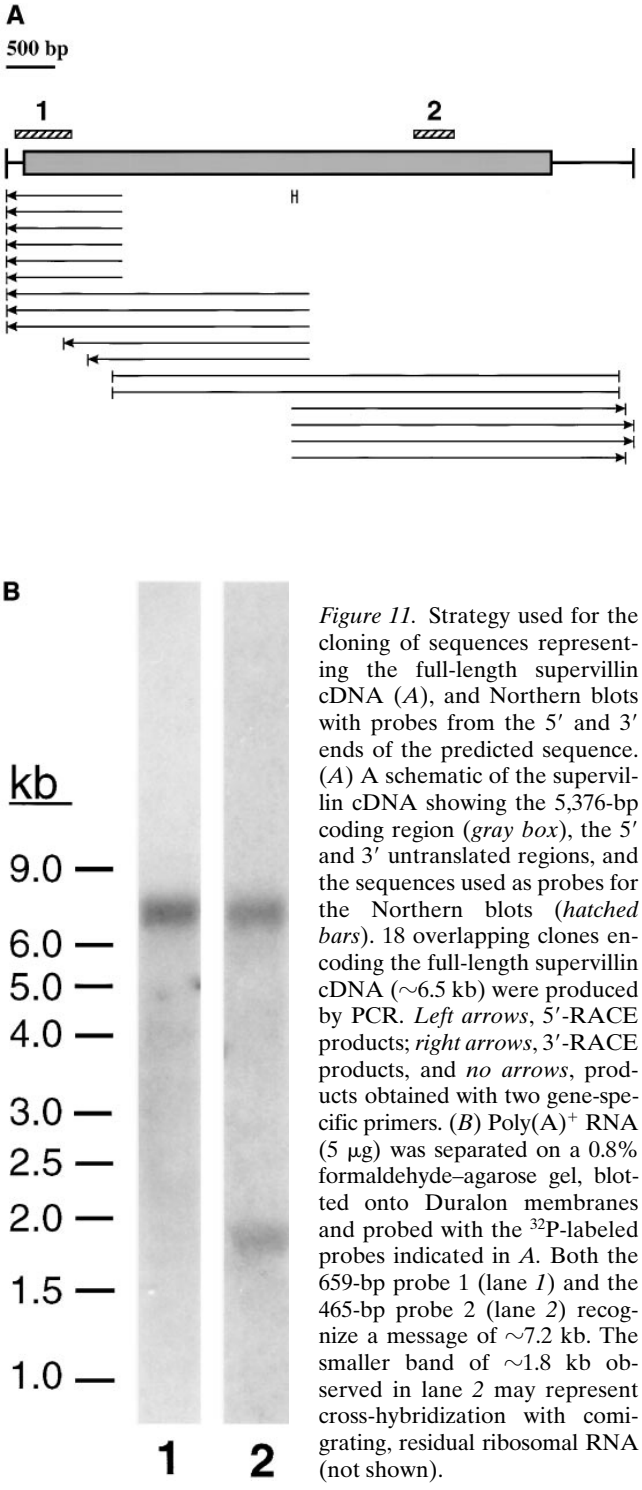

Figure 11. Strategy used for the cloning of sequences representing the full-length supervillin cDNA (*A*), and Northern blots with probes from the 5′ and 3′ ends of the predicted sequence. (*A*) A schematic of the supervillin cDNA showing the 5,376-bp coding region (*gray box*), the 5′ and 3′ untranslated regions, and the sequences used as probes for the Northern blots (*hatched bars*). 18 overlapping clones encoding the full-length supervillin cDNA (~6.5 kb) were produced by PCR. *Left arrows*, 5′-RACE products; *right arrows*, 3′-RACE products, and *no arrows*, products obtained with two gene-specific primers. (*B*) Poly(A)$^+$ RNA (5 μg) was separated on a 0.8% formaldehyde–agarose gel, blotted onto Duralon membranes and probed with the ^{32}P-labeled probes indicated in *A*. Both the 659-bp probe 1 (lane *1*) and the 465-bp probe 2 (lane *2*) recognize a message of ~7.2 kb. The smaller band of ~1.8 kb observed in lane *2* may represent cross-hybridization with comigrating, residual ribosomal RNA (not shown).

oplasmin- and SV40-like nuclear targeting signals (16, 68). Because the nucleoplasmin targeting signal is found in 56% of all nuclear proteins but only ~4% of non-nuclear proteins (25) and because nuclear localization signals are additive (37), the PSORT protein localization prediction program (61) indicates a 96.4% probability that p205 partitions into the nucleus. Hence, an analysis of the p205 primary sequence supports the immunocytological observation of anti-pepA signal within the nuclei of subconfluent cells (Fig. 8, *A* and *C*).

Sequence analysis also suggests a potential mechanism

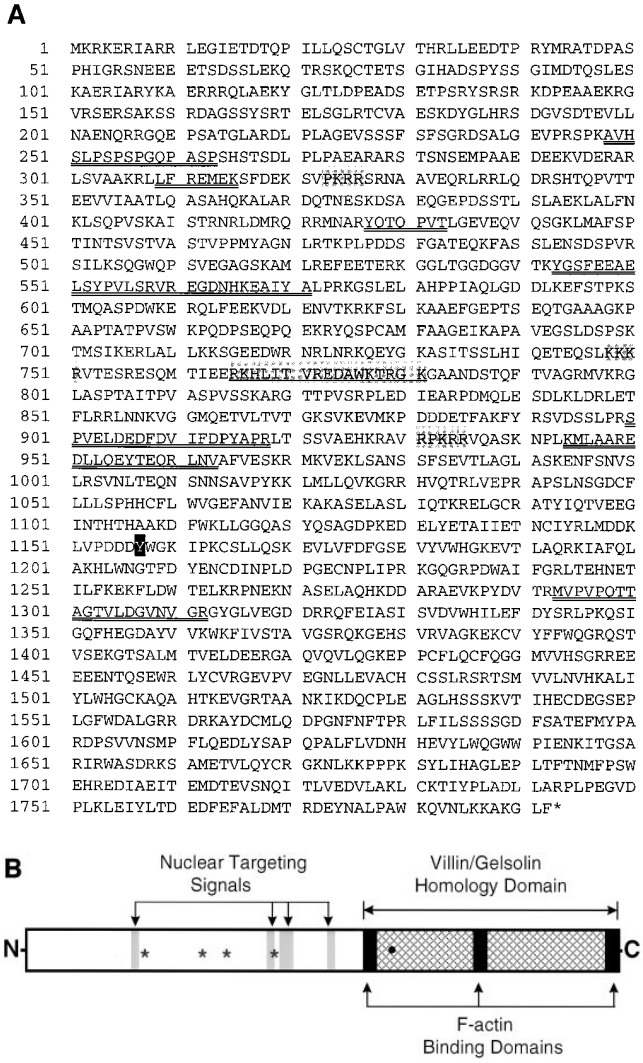

Figure 12. Predicted sequence and domain structure of bovine p205 (supervillin). (*A*) The amino acid sequence starting with the first methionine of the translated ORF includes all eight peptides obtained from purified p205 (*double underline*). The NH_2-terminal half contains four putative nuclear targeting signals (*gray boxes*) the longest of which resembles the nucleoplasmin targeting signal (*single underline*). The COOH-terminal half of the molecule contains a potential tyrosine phosphorylation site (*black*). Amino acid positions are indicated by numbers in the left margin. These sequence data are available from GenBank/EMBL/DDBJ under accession number AF025996. (*B*) Schematic representation of the domain structure showing the NH_2-terminal region with putative nuclear targeting regions (*gray boxes*) juxtaposed with potential protein kinase A phosphorylation sites (*asterisks*). The COOH-terminal domain (*cross-hatched*) shows extensive similarity to villin and gelsolin, with three regions of especially high homology that correspond to potential F-actin–binding sites (*black boxes*). The potential tyrosine phosphorylation site is indicated (·).

for the regulation of p205 accumulation in the nucleus. The putative nuclear localization signals are surrounded by 43 serines and threonines that are potentially phosphorylatable by protein kinase A (Fig. 12 *B*, *asterisks*), protein kinase C, and/or casein kinase II (not shown). Thus, targeting of p205 to the nucleus could be regulated by Ser/Thr phosphorylation, a mechanism documented for other proteins that conditionally localize to the nucleus (37).

The COOH-terminal half of p205 contains 24 potentially phosphorylatable serines and threonines and a consensus site for tyrosine phosphorylation (Tyr-1157; Fig. 12, *A black box* and *B*, *black dot*), protein modifications known to regulate adherens junction structure (3).

The most striking characteristic of the p205 COOH-terminal domain, by far, is its extensive homology (Figs. 12 *B* and 13) with the villin/gelsolin family of cytosolic F-actin–binding proteins (85). Many short stretches of sequence similarity were identified by the BLASTP search algorithm (2) between sequential segments of p205, starting at about Asn-979, through virtually the entire lengths of villin and gelsolin (Fig. 13 *A*). In individual, optimized comparisons of each of these sequences with that of the COOH terminus of p205, the overall percent identities were 29% (villin) and 28% (gelsolin), and the overall similarities were 48 and 50%, respectively.

The nature of the similarity with villin and gelsolin is best appreciated when the percent identities are plotted as a function of position along the length of p205 (Fig. 13 *A*). Regions of very high sequence identity are interspersed with regions exhibiting little or no similarity, usually due to the presence of additional residues in p205. In particular, this analysis identified three localized regions of ~50% sequence identity between p205 and sites in villin and/or gelsolin (Fig. 13, *A* and *B*). Interestingly, two of these sites include sequences that have been previously shown to bind F-actin (85). The first site, amino acids 1,023–1,032, is very similar to a sequence found in the segment-2 region of both gelsolin and villin that, when dimerized, can crosslink actin filaments (23). The second of these sites is the COOH terminus of p205, which is extremely similar to the COOH-terminal "headpiece" region of villin, a sequence involved in bundling actin filaments in vitro (38, 48) and in vivo (32, 35). Interestingly, most of the conserved residues that are required for structural stability or F-actin binding of the villin headpiece (26, 56) are also found in p205 (Fig. 13 *B*, *bottom*), suggesting that this region of p205 also may bind F-actin.

The third region of high sequence similarity between p205, gelsolin, and villin corresponds to COOH-terminal residues in segment five of the latter two proteins (Fig. 13, *A* and *B*). Intriguingly, proteolytic fragments (12) and bacterially expressed proteins (84) containing segments four through six of gelsolin contain an otherwise unmapped Ca^{2+}-dependent site for binding F-actin. It is thus possible that this third region of high homology to villin and gelsolin also corresponds to a sequence that can bind F-actin. In

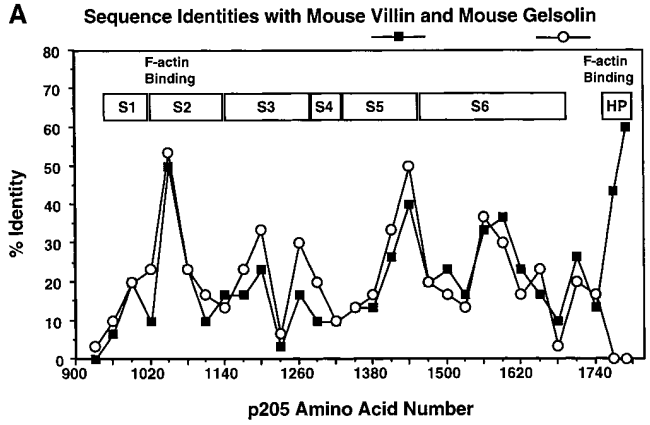

B

Segment 2 Homology Region

Mouse gelsolin	132	VVVQRESQVK GRFVVRATEV PVSWDSFNNG DCFILDLGNN IHQWCGSGSN KFEKLKATQV	191
Mouse villin	133	SDVQRLLEVK GKRNVLAGDV EMSWKSFNRG DVFLLDLGKL IYQWNGPESN RVEKLKGMPL	192
Protovillin	190	AKQYKLEHLK GRRNIRVKQV DISSKSLNSG DVFVLDCEDF IYQWNGSESS RLEKCKGLDL	249
P205	1018	VKKLMLLQVK GRRHVGTRLV EPRAPSLNSG DCFLLDSPHE CLLWVGPAAN VLEKAKASEL	1077
C. elegans ORF	286	VPDVMLHQVK GSKNVQVRLV APAMSSVHEV ACFVWIHQKH LMKKPEGLKS NIEKTKASSL	345

Segment 5 Homology Region

Mouse gelsolin	429	RHSGRQGQLI FNMQGAQSTQ DEVAASAIFT AQLDEELGGT PVQSRVVQGK EPAHIMSLFGG	498
Mouse villin	434	LKEEKGHTLL FTMQGSQASQ DEIAASAYQA VLLDQKYNDE PVQLRVTMGK EPEHIMSIFKG	494
Protovillin	506	AADGSNNSTL FVMQGPESSS EEKGAAALEA KSVGKELHRS CIEVRTVQNK EPNHFLEHFQG	566
P205	1382	RWAGKEKGVV FRMQGRQSTV SEKGTSALVT VELDEERGA. ..QVQVLQGK EPEQFLQCFQG	1439
C. elegans ORF	643	RFTGGSSNIA FVMLGEETIP KGHGLCALRI KETDRT...N SPRIRTADGN EPALFLALFDG	700

Headpiece Homology Region

Chick villin	779	LPRGVDPSKK ENHLSDEDFK AVFGMTRSA FANLPLWKQQ NLKKEKGLF	826
Mouse villin	780	LPEGVDPSKK EEHLSTEDFT RALGMTPAA FSALPRWKQQ NLKKEKGLF	827
Protovillin	912	LENDIDKSCL HEYLSDEEFL STFKMTKSI FQKTPAWKTK QLRVDNGLF	959
P205	1745	LPEGVDPLKL EHYLTDEDFE FALDMTRDE YNALPAWKQV NLKKAKGLF	1792
C. elegans ORF	941	LPAGVDMRKL ESYLTDDDFM KVLKTERSE FYAQKTWKQN DAKKRVGLF	988

Figure 13. Detailed comparison of the COOH terminus of supervillin (p205) with the full-length protein sequences of mouse gelsolin, mouse villin, chicken villin, *Dictyostelium* protovillin, and a predicted *C. elegans* protein (These sequence data are available under GenBank/EMBL/DDBJ accession numbers P13020, M98454, P02640, P36418, and U88311, respectively). (*A*) Mouse villin, mouse gelsolin, and the COOH terminus of supervillin were aligned with PileUp, and the percentage of identical residues in every consecutive 30–amino acid segment of supervillin were plotted vs. the number of the last residue in the segment. The locations of the gelsolin and villin homology segments (*S1–S6*) and the villin headpiece domain (*HP*) are drawn to scale. (*B*) The regions of highest identity between supervillin and the other proteins in this family include portions of segments 2 and 5, which are present in both gelsolin and villin, and the villin headpiece domain, which is absent from gelsolin. Both segment 2 and the villin headpiece contain known actin-binding motifs, indicated by asterisks above the sequence (23, 38, 48). Villin headpiece amino acids implicated in binding to F-actin and in stabilization of headpiece structure (26, 56) are designated by ◆ and ◇, respectively. Identical residues (*black boxes*) and conservative replacements (*gray boxes*), defined as matches scoring ≥0.6 on the Dayhoff matrix (22), are highlighted.

any case, this segment-five homology region in p205, as well as many of the other peaks of sequence identity shown in Fig. 13 *A*, apparently represents an important structural or functional site common to all three of these proteins.

Other proteins exhibiting high structural similarity with p205 are protovillin, a ~100-kD F-actin capping protein from *Dictyostelium* and an open reading frame (ORF) in the *Caenorhabditis elegans* genome that is predicted to encode a ~113-kD protein (Fig. 13 *B*). Optimized alignments along the length of each protein indicate that protovillin is 27% identical (49% similar) and that the *C. elegans* ORF is 25% identical (46% similar) to the p205 COOH terminus. More distant relationships with other members of the villin/gelsolin superfamily, including adseverin, scinderin, severin, and fragmin (85), also were observed (not shown). Thus, at ~200,000 D p205 is the largest member of the villin/gelsolin superfamily. In recognition of this relationship, we propose the name, "supervillin."

Discussion

In this paper, we have identified and characterized a novel plasma membrane–associated, F-actin–binding protein (supervillin/p205), which is present in bovine neutrophils and in various transformed and nontransformed cell lines. We have shown previously that this protein fractionates with crude neutrophil membranes and binds directly and specifically to the sides of α-actin filaments in blot overlay assays (66). We show here that supervillin is a tightly bound peripheral protein (Fig. 2) that can associate with the plasma membranes of both neutrophils (Fig. 1) and MDBK cells (Figs. 8–10). We further show that supervillin can be isolated from neutrophil plasma membranes as part of a high molecular weight complex with endogenous actin (Fig. 5) and that the interaction with actin persists after immunoprecipitation and high stringency washing (Fig. 6). Although many tissue culture cell lines contain both supervillin and another F-actin–binding protein of similar size (Fig. 7 *B*), all of our results to date suggest that supervillin is the only 205-kD F-actin–binding protein in bovine neutrophils. The presence of supervillin in numerous cell lines (Fig. 7) suggests that this protein is one of a small, but growing group of membrane skeleton proteins known to bind actin at the peripheries of many cells (73, 88).

We also show here that the structure of supervillin is novel (Figs. 3, 11, and 12). Not only is this protein currently unrepresented in the protein databases, but it is unique in that it contains both a strong homology to cytosolic actin-binding proteins in the villin/gelsolin family (Fig. 13) and four nuclear localization signals (Fig. 12). The demonstrated tight binding of supervillin to actin filaments (Figs. 1 and 6) is reflected by the prediction from the primary sequence that this protein may contain as many as three binding sites for F-actin (Fig. 13 *B*). Based upon the extent of the sequence similarities and the known properties of the homologous sequences in villin and gelsolin, supervillin may also bundle actin filaments. Interestingly, amino acids required for filament severing in gelsolin (Lys-150 through Gln-160; see reference 41) and villin (Arg-137; see reference 23) are not conserved in supervillin (Fig. 11 *B*), suggesting that, like protovillin (43), supervillin probably lacks this activity. At least one of the F-actin–binding sites in supervillin is insensitive to the presence of free calcium ions since F-actin binding on blot overlays is similar in the presence of either 1 mM EGTA or 0.1 mM $CaCl_2$ (data not shown). However, the definitive determination of the nature of the interaction(s) between supervillin, actin filaments, and calcium ions awaits the identification of a source from which biochemically significant amounts of native supervillin are readily obtainable.

The colocalization of supervillin with E-cadherin at sites of initial (Fig. 8) and established (Fig. 9) cell–cell contact and its internalization with E-cadherin and actin during EGTA-mediated cell dissociation (Fig. 10) suggest that supervillin may be involved in the formation and/or stabilization of actin filament bundles at adherens junctions. Such an activity would be analogous to that documented for villin in the microvilli of highly organized brush borders. Villin both nucleates microvillar assembly in transfected cells and cross-links actin filaments in the mature microvillar core (34). A second precedent may be the actin bundling protein, p30a, which stabilizes filaments against depolymerization (89) and apparently potentiates their association with intercellular junctional membranes, even though p30a does not itself bind tightly to the membrane (30). An even more intriguing paradigm may be α-actinin, an actin-bundling protein that also appears to facilitate the attachment of stress fibers to integrins at focal contacts (64). We hypothesize that supervillin plays an analogous role in actin filament bundling and/or attachment to the membrane at adherens junctions.

Because the COOH terminus of supervillin apparently constitutes the actin-binding domain of the molecule, an attractive hypothetical function for the NH_2 terminus is the targeting of supervillin to appropriate intracellular compartment(s). The localization of supervillin at regions of lateral cell–cell contact (Figs. 8, 9) is quite distinct from the observed concentration of villin in apical microvilli (11, 33). Also, no supervillin is observed in association with the actin filament meshwork at the basal surfaces of MDBK cells. Thus, either the unique supervillin NH_2 terminus or one of the supervillin-specific, "linker" sequences interspersed between the villin/gelsolin homology regions must contain a sequence responsible for targeting to some component of adherens junctions. The punctate cytoplasmic distribution observed in nonadherent cells implies that this target may be membrane associated.

Another intracellular destination for supervillin might be the nucleus. The nuclear localization predicted from the presence of NH_2-terminal targeting signals is supported by the observation that nuclei of low density cells label with an antibody against a supervillin peptide (Fig. 8). Although nuclear localization artifacts are common in fixed cells (57), no significant nuclear staining is observed in EGTA-treated cells (Fig. 10), suggesting that the localization observed in Fig. 8 is not a consequence of our fixation conditions or a fortuitous cross-reaction with a similar epitope in a nuclear protein.

A role for supervillin outside the adherens junction is also suggested by its comparatively high abundance in bovine neutrophils (Figs. 1 and 7 *A*) (66) and HeLa cells (Fig. 7 *B*). These cells are not adherent and either lack (neutrophils) or are grossly deficient (HeLa cells) in classical cadherins detectable by antibodies against the highly conserved cadherin cytoplasmic domain (data not shown). While these cell types might contain a divergent cadherin

with an immunologically distinct cytoplasmic domain (76), it is also possible that supervillin plays different roles in nonadherent and adherent cells. Such a multiplicity of functions is supported by the changing intracellular localization of supervillin as a function of the growth and adhesive state of MDBK cells (Figs. 8 and 9).

Assuming that subsequent analyses with additional antibodies and with epitope-tagged supervillin confirm its multiple intracellular localizations, this protein is an excellent candidate for a signaling molecule that transduces information to the nucleus from the membrane skeleton at sites of cell–cell adhesion. Precedents include β-catenin and the *Drosophila melanogaster* armadillo protein, both of which bind cadherin, potentiate cell–cell adhesion, and function in the Wnt-1/Wingless signal transduction pathway (39, 65). When present at high levels, both β-catenin (6, 58) and armadillo protein (81) can functionally interact with the LEF-1/Tcf family of transcription factors, an interaction that provides one explanation for the apparent involvement of β-catenin in tumor progression (50, 59, 69). Thus, supervillin may be one of a small group of candidate proteins, which also includes the focal contact proteins zyxin and cCRP (70), that could function as relatively direct signaling molecules between the nucleus and the actin cytoskeleton at sites of cell adhesion.

In conclusion, we have shown that supervillin is a novel F-actin–binding protein that cofractionates with endogenous actin, binds peripherally but tightly to neutrophil plasma membranes, and conditionally localizes with E-cadherin at sites of intercellular adhesion. Future work will be directed towards elucidating supervillin function and regulation in adherent vs. nonadherent cells and determining the role of this protein in the modulation of adhesion, motility, and adhesion-mediated signal transduction.

The authors would like to thank C.P. Strassel for production of MDBK cell cDNA and for expert technical assistance. We also thank Dr. J. Leszyk for protein digestion and peptide microsequencing and Dr. J. Aghajanian for electron microscopy of neutrophil membranes and assistance with confocal microscopy. We are also grateful for the assistance of L. Ohrn and M. Martineau for preparation of media/reagents and assistance with laboratory supplies. We also thank Dr. H.G. Hills, Dr. G. Polking, S. Nelson, and W.C. Chu of the Iowa State DNA Sequencing and Synthesis Facility for primer production and automated DNA sequencing.

R.K. Pope was supported by an American Cancer Society postdoctoral fellowship (No. PF-4297), and J.D. Wulfkuhle by a National Institutes of Health (NIH) postdoctoral training fellowship (No. 5T32HD07312-12). This research was supported by NIH grant GM33048 and also benefited from grants to the Worcester Foundation for Biomedical Research from the J. Aron Charitable Foundation, and from the Stork Foundation.

Received for publication 6 June 1997 and in revised form 21 August 1997.

Note Added in Proof. While this paper was in press, Mandai, K., H. Nakanishi, A. Satoh, H. Obaishi, M. Wada, H. Nishioka, M. Itoh, A. Mizoguchi, T. Aoki, T. Fujimoto, et al. (1997. *J. Cell Biol.* 139:517–528) described a 205-kD rat brain cytosolic protein (afadin) that binds to F-actin on blot overlays and exhibits a distribution in epithelial cells similar to that reported here for supervillin. However, the deduced amino acid sequences of supervillin and afadin are not significantly similar, except for the existence of multiple predicted nuclear targeting sequences in both proteins. Thus, afadin is a good candidate for the second ~205-kD F-actin–binding polypeptide that we observe in some cell lines (Fig. 7), but it is not a member of the villin/gelsolin superfamily, nor is it structurally related to supervillin.

References

1. Aberle, H., H. Schwartz, and R. Kemler. 1996. Cadherin-catenin complex: protein interactions and their implications for cadherin function. *J. Cell. Biochem.* 61:514–523.
2. Altschul, S.F., W. Gish, W. Miller, E.W. Myers, and D.J. Lipman. 1990. Basic local alignment search tool. *J. Mol. Biol.* 215:403–410.
3. Anderson, J.M., and C.M. Van Itallie. 1995. Tight junctions and the molecular basis for regulation of paracellular permeability. *Amer. J. Physiol.* 269:467–475.
4. Atkinson, P.H. 1973. HeLa cell plasma membranes. *Methods Cell Biol.* 7: 157–188.
5. Ausubel, F.M., R. Brent, R.E. Kingston, D.D. Moore, J.G. Seidman, J.A. Smith, and K. Struhl. 1989. Current Protocols in Molecular Biology. Vol. 1. John Wiley & Sons, New York.
6. Behrens, J., M.P. von Kries, M. Kühl, L. Bruhn, D. Wedlich, R. Grosschedl, and W. Birchmeier. 1996. Functional interaction of β-catenin with the transcription factor LEF-1. *Nature.* 382:638–642.
7. Bennett, V., and D.M. Gilligan. 1993. The spectrin-based membrane skeleton and micron-scale organization of the plasma membrane. *Annu. Rev. Cell Biol.* 9:27–66.
8. Bjellqvist, B., G.J. Hughes, C. Pasquali, N. Paquet, F. Ravier, J.-C. Sanchez, S. Frutiger, and D.F. Hochstrasses. 1993. The focusing positions of polypeptides in immobilized pH gradients can be predicted from their amino acid sequences. *Electrophoresis.* 14:1023–1031.
9. Borregaard, N., K. Lollike, L. Kjeldsen, H. Sengelov, L. Bastholm, M.H. Nielsen, and D.F. Bainton. 1993. Human neutrophil granules and secretory vesicles. *Eur. J. Haematol.* 51:187–198.
10. Bretscher, A. 1991. Microfilament structure and function in the cortical cytoskeleton. *Annu. Rev. Cell Biol.* 7:337–374.
11. Bretscher, A., and K. Weber. 1979. Villin: the major microfilament-associated protein of the intestinal microvillus. *Proc. Natl. Acad. Sci. USA.* 76:2321–2325.
12. Bryan, J. 1988. Gelsolin has three actin-binding sites. *J. Cell Biol.* 106:1553–1562.
13. Burridge, K., and M. Chrzanowska-Wodnicka. 1996. Focal adhesion, contractility, and signaling. *Annu. Rev. Cell Dev. Biol.* 12:463–518.
14. Burridge, K., T. Kelly, and P. Mangeat. 1982. Nonerythrocyte spectrins: actin-membrane attachment proteins occurring in many cell types. *J. Cell Biol.* 95:478–486.
15. Carraway, C.A.C., and M. Weiss. 1985. Phalloidin shift on velocity sedimentation sucrose gradient centrifugation for identification of microfilament-associated proteins. *Exp. Cell Res.* 161:150–160.
16. Chelsky, D., R. Ralph, and G. Jonak. 1989. Sequence requirements for synthetic peptide-mediated translocation to the nucleus. *Mol. Cell Biol.* 9: 2487–2492.
17. Chia, C.P., A.L. Hitt, and E.J. Luna. 1991. Direct binding of F-actin to ponticulin, an integral plasma membrane glycoprotein. *Cell Motil. Cytoskeleton.* 18:164–179.
18. Chia, C.P., A. Shariff, S.A. Savage, and E.J. Luna. 1993. The integral membrane protein, ponticulin, acts as a monomer in nucleating actin assembly. *J. Cell Biol.* 120:909–922.
19. Condeelis, J. 1993. Life at the leading edge: the formation of cell protrusions. *Annu. Rev. Cell Biol.* 9:411–444.
20. Creighton, T.E. 1984. Proteins: Structures and Molecular Principles. W.H. Freeman and Company, New York. 515 pp.
21. Dahlgren, C., S.R. Carlsson, A. Karlsson, H. Lundqvist, and C. Sjölin. 1995. The lysosomal membrane glycoproteins Lamp-1 and Lamp-2 are present in mobilizable organelles, but are absent from the azurophil granules of human neutrophils. *Biochem. J.* 311:667–674.
22. Dayhoff, M.O., R.M. Schwartz, and B.C. Orcutt. 1978. A model of evolutionary change in proteins. Matrices for detecting distant relationships. *In* Atlas of Protein Sequence and Structure. Vol. 5. M.O. Dayhoff, editor. National Biomedical Research Foundation, Washington DC. 345–358.
23. de Arruda, M.V. Bazari, M. Wallek, and P. Matsudaira. 1992. An actin footprint on villin. *J. Biol. Chem.* 267:13079–13085
24. Del Buono, B.J., F.W. Luscinskas, and E.R. Simons. 1989. Preparation and characterization of plasma membrane vesicles from human polymorphonuclear leukocytes. *J. Cell. Physiol.* 141:636–644.
25. Dingwall, C., and R.A. Laskey. 1991. Nuclear targeting sequences - a consensus? *Trends Biochem. Sci.* 16:478–481.
26. Doering, D.S., and P. Matsudaira. 1997. Cysteine scanning mutagenesis at 40 of 76 positions in villin headpiece maps the F-actin binding site and structural features of the domain. *Biochemistry.* 35:12677–12685.
27. Drenckhahn, D., T. Jöns, R. Koob, D. Kraemer, and S. Wagner. 1992. Role of Na^+, K^+-ATPase and anion exchanger 1 (band 3) as binding sites for the cytoskeleton. *Prog. Cell Res.* 2:263–268.
28. Farrell, R.E., Jr. 1993. RNA Methodologies. A Laboratory Guide for Isolation and Characterization. Academic Press, San Diego. 317 pp.
29. Fechheimer, M. 1987. The *Dictyostelium discoideum* 30,000-dalton protein is an actin filament-bundling protein that is selectively present in filopodia. *J. Cell Biol.* 104:1539–1551.
30. Fechheimer, M., H.M. Ingalls, R. Furukawa, and E.J. Luna. 1994. Association of the *Dictyostelium* 30,000 M_r actin bundling protein with contact regions. *J. Cell Sci.* 107:2393–2401.
31. Firestone, G., and S.D. Winguth. 1990. Immunoprecipitation of proteins.

Methods Enzymol. 182:688–700.
32. Franck, Z., M. Footer, and A. Bretscher. 1990. Microinjection of villin into cultured cells induces rapid and long-lasting changes in cell morphology but does not inhibit cytokinesis, cell motility, or membrane ruffling. *J. Cell Biol.* 111:2475–2485.
33. Friederich, E., C. Huet, M. Arpin, and D. Louvard. 1989. Villin induces microvilli growth and actin redistribution in transfected fibroblasts. *Cell.* 59: 461–475.
34. Friederich, E., E. Pringault, M. Arpin, and D. Louvard. 1990. From the structure to the function of villin, an actin-binding protein of the brush border. *Bioessays.* 12:403–408.
35. Friederich, E., K. Vancompernolle, C. Huet, M. Goethals, J. Finidori, J. Vandekerckhove, and D. Louvard. 1992. An actin-binding site containing a conserved motif of charged amino acid residues is essential for the morphogenic effect of villin. *Cell.* 70:81–92.
36. Furukawa, R., and M. Fechheimer. 1994. Differential localization of α-actinin and the 30 kD actin-bundling protein in the cleavage furrow, phagocytic cup, and contractile vacuole of *Dictyostelium discoideum. Cell Motil. Cytoskeleton.* 29:46–56.
37. Garcia-Bustos, J., J. Heitman, and M.N. Hall. 1991. Nuclear protein localization. *Biochim. Biophys. Acta.* 1071:83–101.
38. Glenney, J.R., and K. Weber. 1981. Calcium control of microfilaments: uncoupling of the F-actin-severing and bundling activity of villin by limited proteolysis in vitro. *Proc. Natl. Acad. Sci. USA.* 78:2810–2814.
39. Gumbiner, B.M. 1995. Signal transduction by β-catenin. *Curr. Opin. Cell Biol.* 7:634–640.
40. Harlow, E., and D. Lane. 1988. Antibodies. A Laboratory Manual. Cold Spring Harbor Laboratory, Cold Spring Harbor, NY. 726 pp.
41. Hartwig, J.H., and D.J. Kwiatkowski. 1991. Actin-binding proteins. *Curr. Opin. Cell Biol.* 3:87–97.
42. Hitt, A.L., J.H. Hartwig, and E.J. Luna. 1994. Ponticulin is the major high-affinity link between the plasma membrane and the cortical actin network in *Dictyostelium. J. Cell Biol.* 126:1433–1444.
43. Hofmann, A., L. Eichinger, E. André, D. Rieger, and M. Schleicher. 1992. Cap100, a novel phosphatidylinositol 4,5-bisphosphate-regulated protein that caps actin filaments but does not nucleate actin assembly. *Cell Motil. Cytoskeleton.* 23:133–144.
44. Hubbard, A.L., and A. Ma. 1983. Isolation of rat hepatocyte plasma membranes. II. Identification of membrane-associated cytoskeletal proteins. *J. Cell Biol.* 96:230–239.
45. Hudson, L., and F.C. Hay. 1980. Practical Immunology. Blackwell Scientific Publications, Boston. 156–202.
46. Ikeda, K., T. Shirao, M. Toda, H. Asada, S. Toya, and K. Uyemura. 1995. Effect of a neuron-specific actin-binding protein, drebrin A, on cell-substratum adhesion. *Neurosci. Lett.* 194:197–200.
47. Ingalls, H.M. 1989. Developmentally-regulated changes in *Dictyostelium discoideum* plasma membrane protein composition and actin-binding activity. Ph.D. thesis. Princeton University, Princeton, NJ. 244 pp.
48. Janmey, P.A., and P.T. Matsudaira. 1988. Functional comparison of villin and gelsolin. Effects of Ca^{2+}, KCl, and polyphosphoinositides. *J. Biol. Chem.* 263:16738–16743.
49. Kartenbeck, J., M. Schmelz, W.W. Franke, and B. Geiger. 1991. Endocytosis of junctional cadherins in bovine kidney epithelial (MDBK) cells cultured in low Ca^{2+} ion medium. *J. Cell Biol.* 113:881–892.
50. Korinek, V., N. Barker, P.J. Morin, D. van Wichen, R. de Weger, K.W. Kinzler, B. Vogelstein, and H. Clevers. 1997. Constitutive transcriptional activation by a β-catenin-Tcf complex in $APC^{-/-}$ colon carcinoma. *Science.* 275:1784–1787.
51. Laemmli, U.K. 1970. Cleavage of structural proteins during the assembly of the head of bacteriophage T4. *Nature.* 227:680–685.
52. Luna, E.J., and A.L. Hitt. 1992. Cytoskeleton-plasma membrane interactions. *Science.* 258:955–964.
53. Luna, E.J., Y.-L. Wang, E.W. Voss, Jr., D. Branton, and D.L. Taylor. 1982. A stable, high capacity, F-actin affinity column. *J. Biol. Chem.* 257:13095–13100.
54. Luna, E.J., K.N. Pestonjamasp, R.E. Cheney, C.P. Strassel, T.H. Lu, C.P. Chia, A.L. Hitt, M. Fechheimer, H. Furthmayr, and M.S. Mooseker. 1997. Actin-binding membrane proteins identified by F-actin blot overlays. In Cytoskeletal Regulation of Membrane Functions. S.C. Froehner, and G.V. Bennett, editors. Rockefeller University Press, New York. 1–18.
55. Matsudaira, P. 1994. Actin crosslinking proteins at the leading edge. *Semin. Cell Biol.* 5:165–174.
56. McKnight, C.J. , P.T. Matsudaira, and P.S. Kim. 1997. NMR structure of the 35-residue villin headpiece subdomain. *Nat. Struct. Biol.* 4:180–184.
57. Melan, M.A., and G. Sluder. 1992. Redistribution and differential extraction of soluble proteins in permeabilized cultured cells. Implications for immunofluorescence microscopy. *J. Cell Sci.* 101:731–743.
58. Molenaar, M., M. van de Wetering, M. Oosterwegel, J. Peterson-Maduro, S. Godsave, V. Korinek, J. Roose, O. Destrée, and H. Clevers. 1996. XTcf-3 transcription factor mediates β-catenin-induced axis formation in *Xenopus* embryos. *Cell.* 86:391–399.
59. Morin, P.J., A.B. Sparks, V. Korinek, N. Barker, H. Clevers, B. Vogelstein, and K.W. Kinzler. 1997. Activation of β-catenin-Tcf signaling in colon cancer by mutations in β-catenin or APC. *Science.* 275:1787–1790.
60. Mottola, C., R. Gennaro, A. Marzullo, and D. Romeo. 1980. Isolation and partial characterization of the plasma membranes of purified bovine neutrophils. *Eur. J. Biochem.* 111:341–346.
61. Nakai, K., and M. Kanehisa. 1992. A knowledge base for predicting protein localization sites in eukaryotic cells. *Genomics.* 14:897–911.
62. Nielsen, B.L., and L.R. Brown. 1984. The basis for colored silver-protein complex formation in stained polyacrylamide gels. *Anal. Biochem.* 141: 311–315.
63. Otey, C.A., M.H. Kalnoski, J.L. Lessard, and J.C. Bulinski. 1986. Immunolocalization of the gamma isoform of nonmuscle actin in cultured cells. *J. Cell Biol.* 102:1726–1737.
64. Pavalko, F.M., and C.A. Otey. 1994. Role of adhesion molecule cytoplasmic domains in mediating interactions with the cytoskeleton. *Proc. Soc. Exp. Biol. Med.* 205:282–293.
65. Peifer, M. 1995. Cell adhesion and signal transduction: the Armadillo connection. *Trends Cell Biol.* 5:224–229.
66. Pestonjamasp, K., M.R. Amieva, C.P. Strassel, W.M. Nauseef, H. Furthmayr, and E.J. Luna. 1995. Moesin, ezrin, and p205 are actin-binding proteins associated with neutrophil plasma membranes. *Mol. Biol. Cell.* 6:247–259.
67. Rivero, F., R. Furukawa, A.A. Noegel, and M. Fechheimer. 1996. *Dictyostelium discoideum* cells lacking the 34,000 dalton actin binding protein can grow, locomote, and develop, but exhibit defects in regulation of cell structure and movement: A case of partial redundancy. *J. Cell Biol.* 135:965–980.
68. Robbins, J., S.M. Dilworth, R.A. Laskey, and Dingwall. 1991. Two interdependent basic domains in nucleoplasmin nuclear targeting sequence: identification of a class of bipartite nuclear targeting sequence. *Cell.* 64: 615–623.
69. Rubinfeld, B., P. Robbins, M. El-Gamil, I. Albert, E. Porfiri, and P. Polakis. 1997. Stabilization of β-catenin by genetic defects in melanoma cell lines. *Science.* 275:1790–1792.
70. Sadler, I., A.W. Crawford, J.W. Michelsen, and M.C. Beckerle. 1992. Zyxin and cCRP: two interactive LIM domain proteins associated with the cytoskeleton. *J. Cell Biol.* 119:1573–1587.
71. Sambrook, J., E.F. Fritsch, and T. Maniatis. 1989. Molecular Cloning. A Laboratory Manual. Cold Spring Harbor Laboratory Press, Cold Spring Harbor, New York. 1-I. 47.
72. Shirao, T. 1995. The roles of microfilament-associated proteins, drebrins, in brain morphogenesis: a review. *J. Biochem. (Tokyo).* 117:231–236.
73. Shuster, C.B., and I.M. Herman. 1995. Indirect association of ezrin with F-actin: Isoform specificity and calcium sensitivity. *J. Cell Biol.* 128:837–848.
74. Shutt, D.C., D. Wessels, K. Wagenknecht, A. Chandrasekhar, A.L. Hitt, E.J. Luna, and D.R. Soll. 1995. Ponticulin plays a role in the positional stabilization of pseudopods. *J. Cell Biol.* 131:1495–1506.
75. Sober, H.A. 1970. Handbook of Biochemistry, Second Edition. The Chemical Rubber Co., Cleveland, Ohio.
76. Suzuki, S., K. Sano, and H. Tanihara. 1991. Diversity of the cadherin family: evidence for eight new cadherins in nervous tissue. *Cell Regul.* 2:261–270.
77. Takeuchi, K., N. Sato, H. Kasahara, N. Funayama, A. Nagafuchi, S. Yonemura, S. Tsukita, and S. Tsukita. 1994. Perturbation of cell adhesion and microvilli formation by antisense oligonucleotides to ERM family members. *J. Cell Biol.* 125:1371–1384.
78. Towbin, H., T. Stahelin, and J. Gordon. 1979. Electrophoretic transfer of proteins from polyacrylamide gels to nitrocellulose sheets: procedure and some applications. *Proc. Natl. Acad. Sci. USA.* 76:4350–4354.
79. Tsukita, S., and S. Yonemura. 1997. ERM (ezrin/radixin/moesin) family: from cytoskeleton to signal transduction. *Curr. Opin. Cell Biol.* 9:70–75.
80. Tsukita, S., M. Itoh, A. Nagafuchi, S. Yonemura, and S. Tsukita. 1993. Submembranous junctional plaque proteins include potential tumor suppressor molecules. *J. Cell Biol.* 123:1049–1053.
81. van de Wetering, M., R. Cavallo, D. Dooijes, M. van Beest, J. van Es, J. Loureiro, A. Ypma, D. Hursh, T. Jones, A. Bejsovec, et al. 1997. Armadillo coactivates transcription driven by the product of the Dorsophila segment polarity gene *dTCF. Cell.* 88:789–799.
82. Volberg, T., B. Geiger, J. Kartenbeck, and W. W. Franke. 1986. Changes in membrane–microfilament interaction in intercellular adherens junctions upon removal of extracellular Ca^{2+} ions. *J. Cell Biol.* 102:1832–1842.
83. Voss, Jr. E.W., 1984. Fluorescein Hapten: An Immunological Probe. CRC Press, Inc., Boca Raton, FL. 193 pp.
84. Way, M., J. Gooch, B. Pope, and A.G. Weeds. 1989. Expression of human plasma gelsolin in *Escherichia coli* and dissection of actin binding sites by segmental deletion mutagenesis. *J. Cell Biol.* 109:593–605.
85. Weeds, A., and S. Maciver. 1993. F-actin capping proteins. *Curr. Opin. Cell Biol.* 5:63–69.
86. Wuestehube, L.J., and E.J. Luna. 1987. F-actin binds to the cytoplasmic surface of ponticulin, a 17-kD integral glycoprotein from *Dictyostelium discoideum. J. Cell Biol.* 105:1741–1751.
87. Yamada, K.M., and S. Miyamoto. 1995. Integrin transmembrane signaling and cytoskeletal control. *Curr. Opin. Cell Biol.* 7:681–689.
88. Yao, X., L. Cheng, and J.G. Forte. 1996. Biochemical characterization of ezrin-actin interaction. *J. Biol. Chem.* 271:7224–7229.
89. Zigmond, S.H., R. Furukawa, and M. Fechheimer. 1992. Inhibition of actin filament depolymerization by the *Dictyostelium* 30,000-D actin-bundling protein. *J. Cell Biol.* 119:559–567.